Université Abou Moumouni

Doctoral Research Program on Climate Change and Energy

(DRP-CCE)

NIGER

INTERNATIONAL MASTER PROGRAM

IN RENEWABLE ENERGY AND GREEN HYDROGEN

SPECIALITY: PHOTOVOLTAICS FOR GREEN HYDROGEN TECHNOLOGY

MASTER THESIS

Topic:

Indoor LED charging of batteries with organic solar modules

Presented by: **KONE Bakary on 28/09/2023**

Examen committee Members

Chair: Ass. prof. Bruno Korgo Senior Lecturer at Joseph Ki-Zerbo University, WASCAL Regional Coordinator for Renewable Energies and Green Hydrogen (Burkina Faso)

Examinator: Dr. Inoussa Abdou Saley, University Abdou Moumouni- Niger

Main supervisors: Dr. Merdzhanova, Tsvetelina, Forschungszentrums Julich-Germany

Dr. Astakhov,Oleksandr Forschungszentrums Julich-Germany

Prof. Uwe Rau Forschungszentrums Julich-Germany

Local supervisors: Dr. Abdoulkadri Ayouba Mahamane, University Abdou Moumouni- Niger

Dr. Hassane Adamou, University Abdou Moumouni- Niger

Academic year 2022-2023

Dedication

I dedicate this thesis:

To my dear parents and my dear uncle for their love and support throughout my studies.

To my dear brothers for their encouragement and moral support.

To my dear sisters for their support and encouragement.

To all my family and friends for their support throughout my university career.

ACKNOWLEDGEMENTS

I would like to thank the German Federal Ministry of Education and Research BMBF, the West Africa Science center for Adaptable Land use (WASCAL), for their funding of this program.

My thank go out to:

Prof. ADAMOU Rabani (Director of WASCAL Doctoral Research Programme on Climate Change and Energy), Ass. Prof. INOUSSA Maman Maarouhi (Coordinator and Deputy Director of Wascal DRP-CCE), Ass. Prof. MOUNKAILA SALEY Moussa (Scientific Coordinator Wascal DRP-CCE) and Dr AYOUBA MAHAMANE Abdoulkadri (Coordinator IMP-EGH Program, Wascal DRP-CCE).

I address my thanks to the people who helped me in the realization of this Master's thesis.

First of all, I thank Doctor Professor Uwe Rau director of the IEK-5 Photovoltaic Institute Forschungszentrums Jülich Germany for his excellent supervision during this internship.

I am very grateful to my supervisors Doctor Merdzhanova Tsvetelina and Doctor Astakhov Oleksandr who were next to me and always available for the correction and proofreading of this document.

I would like to express my thanks to my two supervisors Dr. Abdoulkadri Ayouba Mahamane and Dr. Hassane Adamou, for the work they have done to improve this work.

I thank Mr. Christoph Zahren for the calibration of the solar simulator and LED simulator devices finally for realizing my experiments and also Mr. Li-Chung King for his support during the experimental study. I would particularly like to thank all the staff at the Institute Photovoltaic IEK-5 of Forschungszentrums Jülich Germany for their support.

I will not forget to address all my thanks to the dynamic staff of Wascal DRP CCE Niger.

ABSTRACT

Energy harvesting inside buildings has received increasing attention as a way to improve the durability and battery life of electronic devices by harnessing ambient light sources. Organic solar modules offer unique advantages, such as flexibility, lightweight, and tunability, making them an attractive candidate for indoor energy harvesting applications. This thesis studies the feasibility of using organic solar modules for charging batteries by LED at 300-500 Lux under the condition of the different spectrum inside the house and in the office. Battery charging tests were performed to analyze the relationship between light intensity, efficiency of organic solar modules and battery charging capacity in indoor applications for charging electronic devices and miscellaneous under low light intensity. In this study, we demonstrated the possibility of charging a sodium anion battery coupled directly to an organic photovoltaic system under a 300-500 Lux LED corresponding to a light power density of 0.107-0.284 mW/cm^2.The efficiency of the organic photovoltaic in this range was 4.98% and the efficiency of the PV-to battery was 3.25% and the overall efficiency was 3.07% under an LED light power density of 0.107-0.284 mW/cm^2. With the different results we have obtained, and the success of the experiment, recharging electronic devices under indoor lighting with organic photovoltaic cells is feasible.

Keywords: indoor LED lighting, organic photovoltaics, sodium-ion battery.

RÉSUMÉ

La collecte d'énergie à l'intérieur des bâtiments a fait l'objet d'une attention croissante en tant que moyen d'améliorer la durabilité et l'autonomie des appareils électroniques en exploitant les sources de lumière ambiantes. Les modules solaires organiques offrent des avantages uniques, tels que la flexibilité, la légèreté et l'adaptabilité, ce qui en fait un candidat intéressant pour les applications de collecte d'énergie en intérieur. Ce mémoire étudie la faisabilité de l'utilisation de modules solaires organiques pour le chargement des batteries par LED à 300-500 Lux sous différentes conditions de spectres d'intérieure de la maison et dans le bureau. Des tests de charge de la batterie ont été effectués pour analyser la relation entre l'intensité lumineuse, l'efficacité des modules solaires organiques et la capacite de charge de la batterie dans l'application intérieur pour charger des appareils électroniques et divers sous une faible d'intensité de la lumière. Dans cette étude, nous avons démontré la possibilité de charger une batterie à ion sodium couplée directement à un système photovoltaïque organique sous éclairement LED 300-500 Lux correspondant à une densité de puissance de lumière de 0.107-0.284 mW/cm^2. L'efficacité du photovoltaïque organique dans cet intervalle est de 4.98% et l'efficacité de la charge de la batterie est 3.25%. L'efficacité globale est de 3.07%, sous une densité de puissance de lumière LED de 0,107-0,284 mW/cm^2. Avec les différents résultats obtenus et le succès de l'expérience, la recharge d'appareils électroniques sous éclairage intérieur avec des cellules photovoltaïques organiques est réalisable.

Mots clés : éclairage LED intérieur, photovoltaïque organique, batterie sodium-ion.

.

ACRONYMS AND ABBREVIATIONS

WASCAL: West African Science Service Center on Climate Change and Adapted Land Use

BMBF: German Federal Ministry of Education and Research

OPV: Organic Photovoltaic

OSC: Organic Solar Cell

LED: Light Emission Diode

AM1.5G: Air mass 1.5 global spectrum

STC: standard test condition

IOT: internet of Thing

EQE : External quantum efficiency

IQE : Internal quantum efficiency

BHJ: Bulk Hetero junction

I-V: current voltage

ŋ: Efficiency (%)

FF: Fill Factor (%)

V: Applied Voltage (V)

I_{sc}: Short-circuit current (mA)

V_{oc}: Open-circuit voltage (V)

R_s: series resistance (Ω)

R_{sh}: Shunt resistance (Ω)

MPP: maximum power point (mW)

I_{mpp}: current at maximum power point (mA)

V_{mp}p: voltage at maximum power point (V)

J_{sc}: short-circuit current density (mA/cm^2)

I_{ph}: Photo current (mA)

I_{sh}: shunt current (mA)

I_o: Diode reverse saturation current

R_L: Resistance Load

n: Diode ideality factor

Vs: Versus

ITO: indium tin oxide

PEDOT: PSS Poly(3,4-ethylenedioxythiophene) polystyrene sulfonate.

PCPDTBT: Poly(4,4-dialkyl-cyclopenta[2,1-b:3,4-b’] dithiophene-alt-2,1,3-benzothiadiazole)

PCBM: 6,6-Phenyl-C_{61}-butyric acid methyl ester

CBA: indene C_{60} Bisadduct

P3HT: Poly 3-hexyle thiophene

DPPTT: DPPTT: Poly[2,5-(2-octyldodecyl)-3,6-diketopyrrolopyrrole-alt-5,5-(2,5-di(thien-2-yl) thieno [3,2-b] thiophene)]

PTB7: Poly[[4,8-bis[(2-ethylhexyl) oxy] benzo[1,2-b:4,5-b’] dithiophene-2,6-diyl] [3-fluoro-2-[(2-ethylyhexyl) carbonyl] thieno[3,4-b] thiophenediyl]].

LIST OF TABLES

LIST OF FIGURES

TABLE OF CONTENTS

INTRODUCTION

1. Background

Energy is considered to be one of the main challenges to the long-term growth of human cultures. Environmentally-friendly renewable energy sources, which offer an alternative to traditional fossil fuels, have undergone significant development in recent decades due to their ability to produce energy without emitting greenhouse gases and thus mitigate climate change caused by global warming. Photovoltaic systems, which convert sunlight directly into electricity, account for a large and growing share of the world's capacity to produce electricity from alternative energies (Li, et al., 2021).

Many electronic devices, such as wireless sensors, IoT devices, wearable gadgets, and portable electronics, operate indoors and rely on batteries for power. Traditional methods of charging batteries often involve hard-wired connections to power sources, which can be impractical, inconvenient, or aesthetically unappealing in some indoor environments. Some variety of energy storage batteries are restricted by limited operational lifetime and long charge time. Indoor organic photovoltaic could be the solution to power these electronic components.

Improving of organic photovoltaic for the recycling of indoor lighting in our homes and offices may be a solution to increase energy demand in the future. The organic photovoltaic is the photovoltaic device which use the organic material to convert sunlight or other light to produce electricity. Light emission diode (LED) is a type of solid-state lighting technology and have become increasingly popular due to their energy efficiency, long life and versatility. Indoor applications of organic photovoltaic have received increasing attention in recent years due to their unique properties, such as superior performance compared to silicon solar cells under indoor lighting, better operational stability under LED or fluorescent lighting compared to outdoor irradiation, high compatibility with indoor portable devices and high flexibility. (Xu, et al., 2021).

Energy stored in the battery in a photovoltaic-battery (PV-battery) device illuminated by the indoor LED light can be reused as needed in variety of small-scale electronic devices.

2. Motivation

This work aims to explore applicability and potential of Organic photovoltaic (OPV) for indoor light harvesting and to determine the characteristics of an OPV under different conditions of indoor LED light. Test feasibility of direct PV-battery charging under low LED light corresponding to typical indoor environment.

3. Problem statement

This research project is directed towards the development of scientific reasoning on indoor photovoltaic application with organic solar module for battery charging.

The problem addressed in this research project is the need to find a viable and sustainable energy solution for indoor applications, focusing on battery charging. In fact, traditional photovoltaic cells are generally used for outdoor applications for the production of energy and their performance is limited in indoor applications due to the low intensity of the indoor and the different spectral distribution. Various thin-film silicon as well as perovskite technologies have all improved efficiencies under indoor illumination with LED lightning (Agbo, et al., 2017) and substantially higher band gaps than crystalline Silicon. With the increasing use of indoor LED lighting, it appears that the LED output spectrum matches perfectly with the absorption spectrum of lead halide perovskite solar cells and hydrogenated amorphous silicon. Therefore, the LED light will be efficiently harvested or absorbed from these solar cells in contrast to AM1.5 spectrum.

The research will be based on determining the potentials of organic solar cell technology to operate under low light intensity LED lighting and the capability for direct charging of a battery will be investigated. Organic photovoltaic is considered to perform well in indoor conditions because of its cleanliness, flexibility, lightweight, and low-cost manufacturing it can be used in the indoor environment to produce energy and charge the battery. In this project, we will determine the performance of the organic solar modules for harvesting indoor light and indoor applications.

4. Research Question

The research question will be as follows:

What is the potential of organic photovoltaic for indoor applications?

What is the performance of organic photovoltaic modules directly coupled to Na ion batteries to power indoor devices?

5. Research Hypotheses

- Organic photovoltaic can charge the battery in under low light emitted by a typical white light emitting diode (LED) light.
- The combination of OPV with battery can provide power for IoT devices indoors.

- The artificial light can play a double role, not only it can illuminate the interior of the house for the needs, but also this light can be recycled using photovoltaic system.

6. Objectives:

The main objective is to evaluate the indoor light-emitting diode (LED) for charging sodium anion batteries with organic solar modules.

Specific objectives:

- Determine the I-V characteristics and PV parameters of organic solar module under one Sun.
- Determine the I-V characteristics and PV parameters of organic solar module under LED lighting and special attention will be given to the range of 300-500 lux.
- Charge sodium ion Na Battery under LED lighting at 300-500 lux.
- Estimate the solar-to-battery efficiency as well as the overall efficiency of charging. of a Na ion battery with OPV module under LED lighning in the range 300-500 lux.

7. Structure of the thesis

This study is made up of three main chapters preceded by a general introduction and ends with a conclusion. It is organized as follows: The introduction supplies the necessary background or context for our research problem. Then, the first chapter is the literature review part. Afterward, the second chapter highlights the materials and methods used in this study while the last chapter presents the results and discussion.

CHAPTER 1: LITERATURE REVIEW

1.1. Photovoltaics application

Photovoltaic technologies are currently used for outdoor applications, such as traditional solar power plants, solar home systems on roofs and street lighting, but also for other uses such as low-energy electronic devices (Xie, et al., 2021). Indoor photovoltaics hold great promise as an autonomous power source for internet of things (IoT) devices. The rapid increase in demand for low-power for IoT devices for indoor applications is not only accelerating the development of high-performance indoor photovoltaic application, but is also encouraging the electronics and semiconductor industries to design and build ultra-low-power devices for powering internet of things systems (Jahandar, et al., 2021). According to Ben *et al*., a useful natural energy source is photovoltaic PV solar energy, since the early part of the 1970s, indoor photovoltaic applications have been widely used in commercial settings (Ben, et al., 2014).

The development of new indoor photovoltaic materials and devices with suitable absorption spectra, large open-circuit voltages with low energy loss, reduced trap-mediated charge recombination and leakage currents, and device stability under indoor conditions are some of the key issues for optimizing indoor photovoltaic materials and devices different from those under 1 sun condition (Ge, et al., 2021). As shown on the **Figure 1.1** the various benefits of indoor photovoltaic applications will be considerable in the future for low power consumption devices, where the organic solar module is applied to convert light from the LED light source in the home or office into electricity to charge the battery of electronic devices that have a low power of 1 nW to 10 W, as shown in the **Figure 1.1** at right.

Figure 1.1: Indoors Photovoltaic application (left) a future house with OPV thermostat, computer mouse, remote control, curtains, lampshades and coffee table mats for re-using indoor light; and (right) power requirements for various devices used indoors and power from a 1 cm ^{2} OPV cell (L. Cutting, et al., 2016).

1.2. Organic photovoltaics - principal and design:

Organic photovoltaic (OPV) solar cells have a great potential for next-generation photovoltaic technology due to their light weight, semi-transparent properties, and low-cost solution processes. The high conversion efficiency has been achieved with OPV solar modules but there are still challenges in outdoor applications due to solar radiation, high temperature and large-scale manufacturing. (Cui, et al., 2020). According to Scharber *et al* (Sharber et al., 2013) the absorber layer of an efficient bulk heterojunction organic solar cell is made up of so-called donor and acceptor molecules. Donors are usually conjugated polymers, oligomers or pigments, while acceptors are often fullerene derivatives. These materials are classified as organic semiconductors. **Figure 1.2** shows the chemical structure organic solar cell based on polymer and fullerenes.

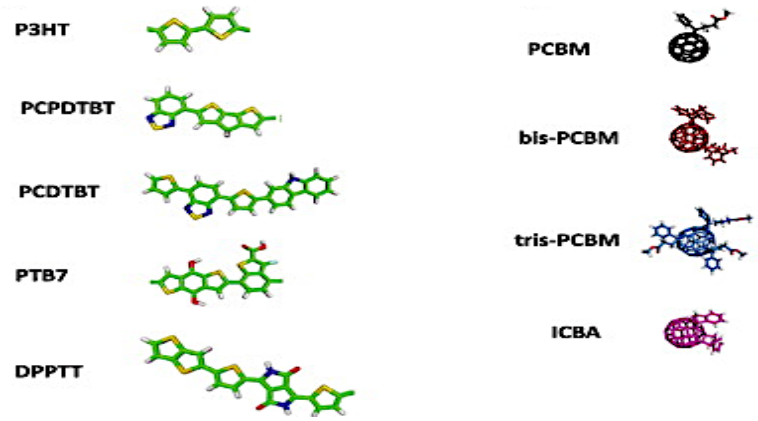

Figure 1.2 : Structure and chemical composition of Organic photovoltaic cells (a) chemical structure backbones of polymer P3HT, PCPDTBT, PCDTBT, PTB7, DPPTT, (b) chemical structure of fullerenes PCBM, bis-PCBM, tris-PCBM, ICBA (Nelson, 2011).

The main power conversion steps in operation of organic photovoltaics are made up of three parts, absorption, charge separation and current collection as explained by kondolot, *et al*., as described in the **Figure 1.3**.

Absorption: the organic components in the OPV cell's active layer absorb photons and produce electron-hole pairs when light is shined on them. The interaction of photons with the organic semiconducting components in the active layer of the cell is what causes light to be absorbed in an OPV cell.

Charge separation: within the active layer, there is a built-in electric field that keeps the electron-hole pairs apart, the active layer's donor and acceptor materials have different energy levels, which results in the creation of this electric field.

The electrical output current generation: the charge separation and collecting procedures provide the electrical output of an OPV cell (Kondolot, et al.,2023). According to *Goo et al*., organic photovoltaic is one of the photovoltaic cell technologies that offer the best performance 13.9% in terms of energy conversion indoors, with a high absorption coefficient and tunable absorption. The photoactive layer makes for efficient absorption in low light conditions (Goo, et al., 2018). According to Kim *et al*., solar cells based on conjugated polymers and fullerenes offer an opportunity as a renewable energy source in the same context organic tandem cell gives 6.7% efficiency (Kim, et al., 2007). **Figure 1.3** details the principal working of Organic photovoltaic.

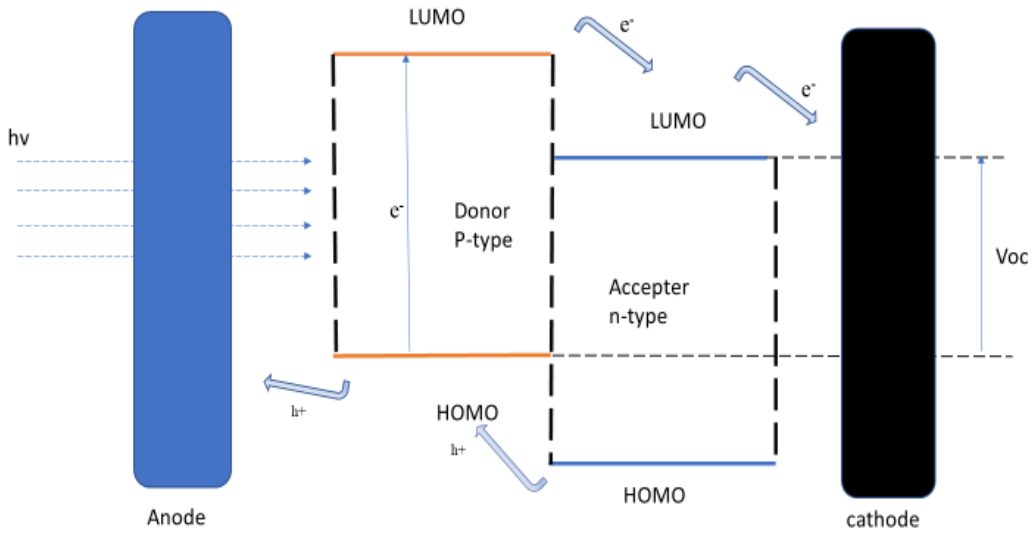

Figure 1.3 : Principle of working of organic photovoltaic (Kondolot, et al.,2023).

For Reinder *et al.*, to create asymmetry and drive electron flow in the low work function interlayer and hole flow in the opposite direction, the hole and electron collecting interlayer has varying work functions. The direction absorber can be one-layer, numerous layers, or a combination of organic materials. The energy levels for electrons and holes are represented by LUMOA and HOMO. (Reinders , et al., 2017). Organic solar photovoltaic was fabricated on cellulose nanocrystalline (CNC) substrates with CNC/Ag (20 nm) polyethyleneimine ethoxylated (PEIE)/active layer/MoO_3/Ag structure, giving a power conversion efficiency of

2.7%. Substrates such as glass, plastic, metal foil and paper are suitable for Organic photovoltaic manufacturing because of their very low manufacturing costs (Zhou, et al., 2014). **Figure 1.4** presents the architecture structure of bulk hetero junction organic solar cell in which the active layer consitued the donors and acceptors. (a) Standard device design with the cathode on top of the device stack and (b) inverted device architecture with the cathode located on the transparent substrate. The **Figure 1.5** depicte (a) A cross-sectional schematic illustration of an organic solar cell. (b) A graphic showing the solar cell's corresponding energy levels when illuminated.

a) b)

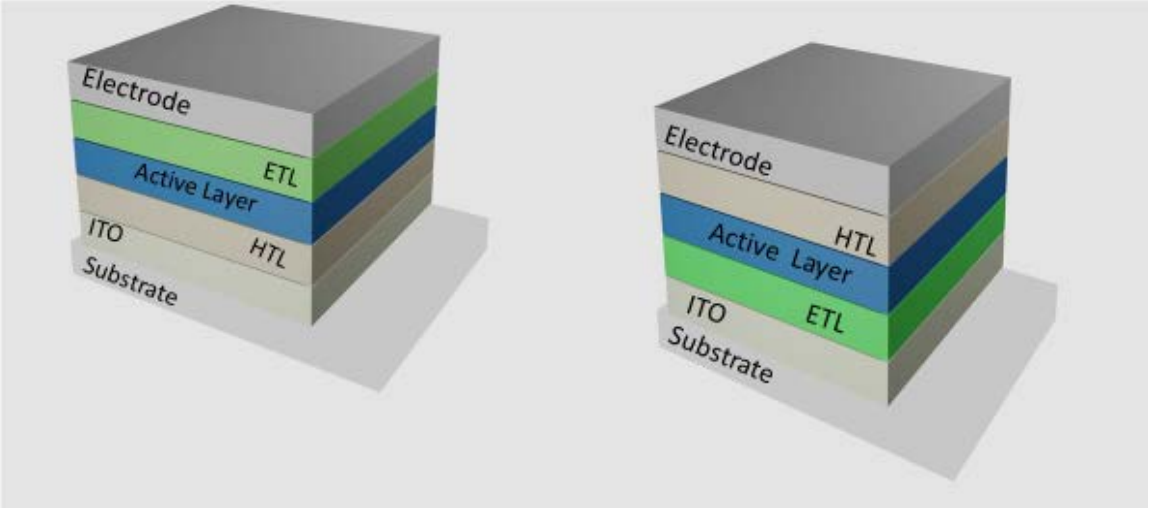

Figure 1.4 : Different architecture of bulk hetero junction device organic solar cell.

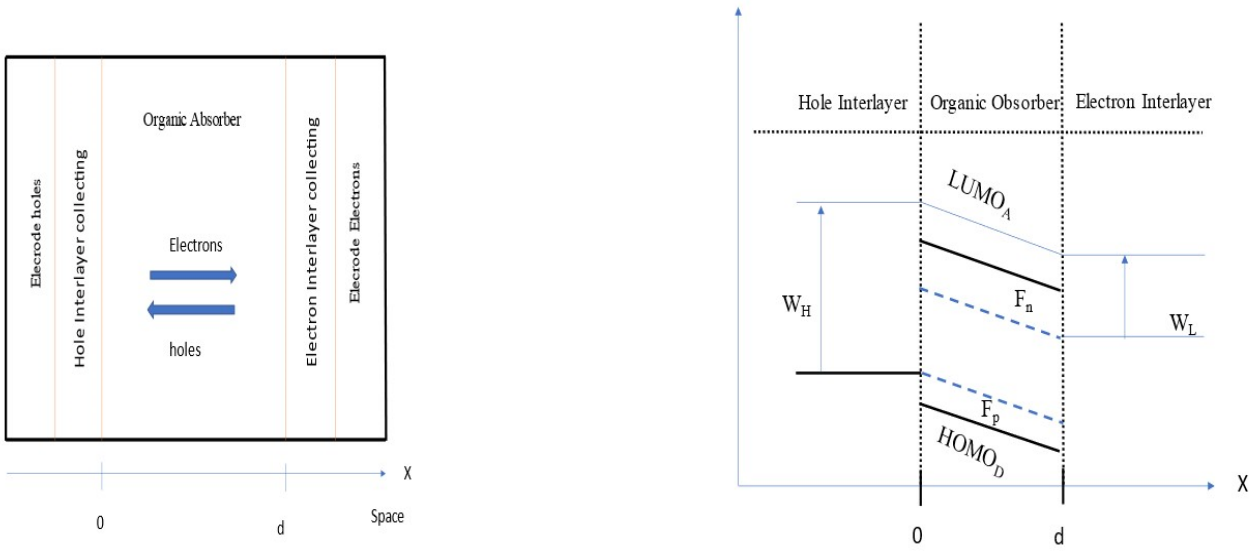

Figure 1.5: (a) A cross-sectional schematic illustration of an organic solar cell. (b) A graphic showing the solar cell's corresponding energy levels when illuminated (Kondolot, et al.,2023).

The introduction of BDT units into photovoltaic polymer design was for the first time in 2008 (Yao, et al., 2016) . A number of high-performance organic photovoltaics have been developed in recent years, including the following poly [2,6-(4,4-bis-(2-ethylhexyl)-4H-cyclopentan[2,1-b;3,4-b'] dithiophene)-alt-4,7-(2,1,3-benzothiadiazole)] (PCPDTBT), a low-bandgap polymer with absorption up to 900 nm. Organic solar cells made from this polymer showed an initial efficiency of around 3%. However, by incorporating alkanedithiol-based additives, the researchers were able to achieve yields of the order of 5.5% (Li, et al., 2012). Organic photovoltaic made with a photoactive layer poly(3-hexylthiophene-2,5-diyl): indene-C60 bisadduct (P3HT: ICBA) based on electron collecting interlayer ZnONPs/PEIE (0,4% by weight) gave a good performance of 14,1±0,3% under a 1000Lux LED lamp. (Shin, et al., 2019).

1.3. Organic photovoltaics for indoors light Harvesting under LED spectrum

The light outdoor which corresponded to sun light and characterized by AM1.5 spectrum is represented by its power density. Indoor illuminated conditions are usually characterized by the human eye specific illuminance measured in lux (lx) which is essentially the light power density multiplied by the photopic sensitivity of a human eye. The efficiency and output power of module depend of irradiance. Depending on the type of light source and its distance, the light intensity under artificial lighting settings in offices and industries is often less than 5

W/m^2, as opposed to 100–1000 Wm^{-2} under outdoor lighting conditions. In fact, the human eye can only detect light in a narrow range of wavelengths, from 380 violet to 780 nm red, while the standard AM 1.5G solar spectrum is defined as the range from 280 nm to 4000 nm (Minnaert, et al., 2014). As reported by Yin *et al.*, the organic materials have a great strong absorption in the region of the visible light between 300-760 nm for that the OPV are classified as better capture of the light than the photovoltaic with bases of silicon (Yin, et al., 2018). According to Lechêne *et al.*, the artificial indoor lighting is classified into three spectrum categories: incandescent solar bulbs, such as compact fluorescent high-temperature lamps (CLF) and LED. Indoor light intensity varies according to the type of room, the position of orientation and the proximity of the light source. Indoor illumination ranges are defined as low illumination (0 to 200 lx), typical illumination (200-500 lx) and excellent illumination superior to 500 lx (Lechêne, et al., 2016).

Light intensity ranges from 500 to 2000 lux, enabling light intensities of less than $1mW.cm^{-2}$ to be obtained. On the other hand, simulated AM1.5G illumination of 100 $mWcm^{-2}$ is less than 100 times more intense than the light used in everyday life (Opoku, et al., 2022). According to Lee *et al.*, the development of strategies for efficiently converting energy from indoor light into electricity is advanced. Given that the luminous intensity of indoor light sources (0.1-1 mWm^{-2}) is to 100 times lower than that of the sun, and emission spectra are relatively narrow 400-700 nm, the organic photovoltaic is considered ideal for indoor applications due to its power conversion efficiency and mechanical properties of flexibility and extensibility (Lee, et al., 2023) . For Cutting *et al.,* work states that it is possible to achieve a power conversion of over 20% in organic photovoltaics under white LED light, which corresponds to the power conversion of polycrystalline silicon and is comparable to that of amorphous silicon and copper indium gallium selenide (CIGS) photovoltaic cell (Cutting, et al., 2016). According to Mori *et al.,* the emission spectrum of the LED extends from 400 to 800 nm, which corresponds to the range of the EQE curve of the Organic photovoltaic. As a result, the difference in Jsc between c-Si-SC and OSC became much smaller under LED illumination than under solar illumination, as both solar cells are sensitive to all wavelengths of photons emitted by the LED. Organic photovoltaic materials suitable for indoor applications could be developed (Mori, et al., 2015). In 2015, the performance of OPV and silicon solar cell was studied by the researchers Yang *et al.*, under LED irradiation and compared to silicon solar cell. The power conversion of Organic solar cell was found to be 21.3% under LED light. (Yang, et al., 2017). **Figure 1.7** represents the different spectrum of light and the bandgap of different solar cell. In (a): standard solar

spectrum AM1.5G, spectrum with LED and the spectrum CFL. In (b): Maximum efficiencies as a function of bandgap for different photovoltaic modules under white LED light and thus under CFL light are studied by Mathews *et al.*, (Mathews, et al., 2019). It has report by Kin *et al.*, that the maximum power conversion of wide-band lead halide perovskite solar module of 43,9% under LED concentrated illumination (24.5 mW/cm^2 and 31% under 500 Lux (Kin, et al., 2022).

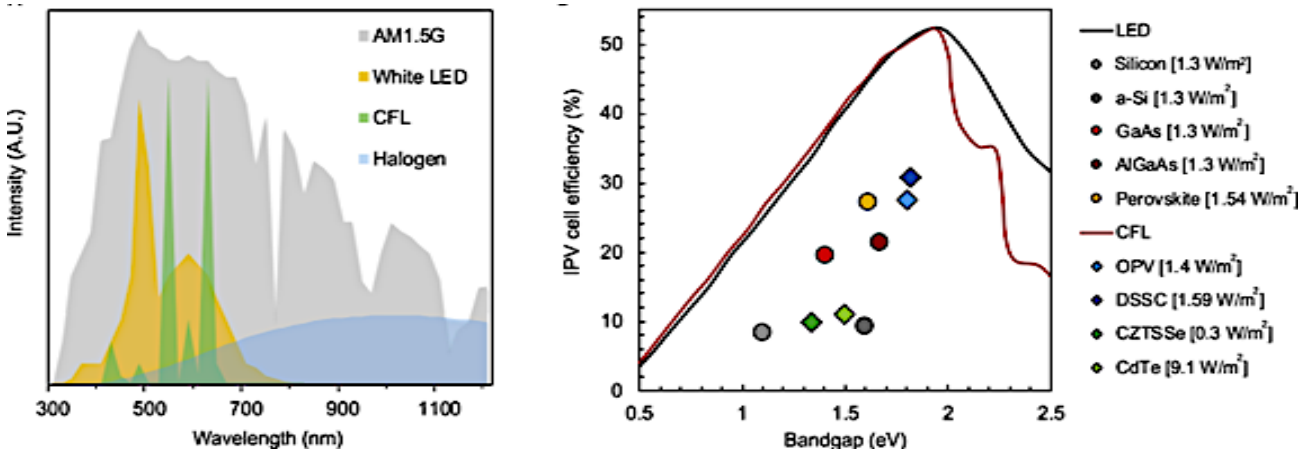

Figure 1.6: Spectrum and maximum efficiencies as a function of bandgap for different photovoltaic modules (Kin, et al., 2022).

1.4. Battery Coupled to OPV module and charging under LED irradiance:

Integrating a self-recharging battery into small planar and mobile objects (e.g., cell phones, smart cards, remote controls, labels, etc; could revolutionize their use. This could be achieved by coupling batteries to small, independent sources of electrical energy, such as the solar cells we need to power our electronic devices (Dennler, et al., 2007). According to Kin *et al.* 2022, the combination of photovoltaic devices integrated with a rechargeable battery represents a viable strategy for powering devices such as wireless sensors and sensor arrays, as well as in locations where weight and size are paramount, such as satellites (Kin, et al., 2022). Direct integration of collection and storage offers the advantage of miniaturisation. The use of efficient high-voltage solar cells is essential for adapting current batteries to achieve greater charging efficiency (Kin, et al., 2020). The integrated battery device with a photovoltaic module for charging and discharging the battery is explained by Hoefler *et al.*, example was taken by organic tendam cell, they report that when the organic tandem solar cell is illuminated, the photo rechargeable battery is theoretically directly charged and discharged on external load outside force. The photovoltage produced by the organic tandem solar cell should be able to apply an overvoltage to the solar battery in order to charge it. (Hoefler, et al., 2020).

Operation of a PV-battery device is illustrated as a power flow block diagram in **Figure 1.7 (a)** and circuit diagram of a directly coupled PV-battery device connected to a load is presented in **Figure 1.7 (b)**. In a PV module the power of light ($P_{L)}$ is converted into electric power (P_{PV}), which is then split into power used by a load ($P_{L)}$ and power used to charge batteries (P_{Bc}). When the PV module is inactive in the dark, a blue arrow indicates that the battery P_{Bd} powering the load With sufficient irradiation, the blue arrows indicate currents in the dark. I_{PV}: PV module current; I_L: current through the load; I_B: battery current; R_L: equivalent load resistance (Astakhov, et al., 2020).

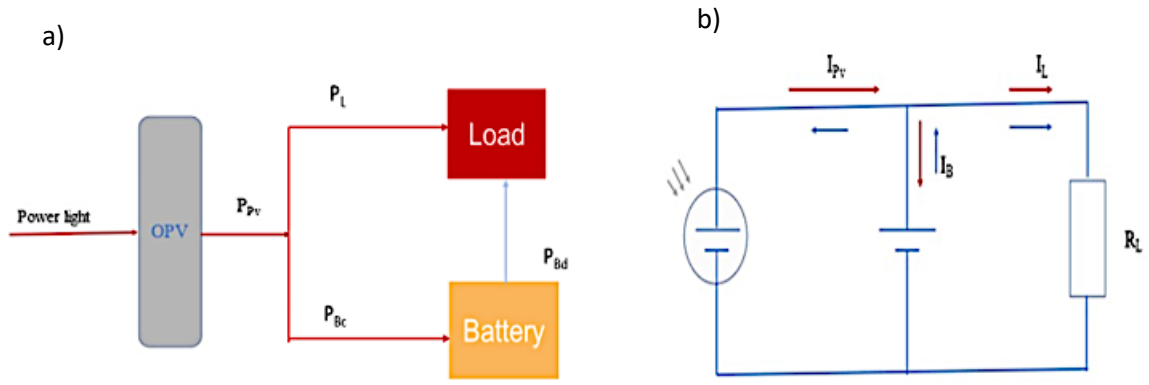

Figure 1.7: a) OPV module coupled with a high-capacity sodium-ion battery. b) Circuit diagram of directly couple PV-battery device.

CHAPITER 2: MATERIALS AND METHODOLOGY

This work has been realized in the research center “Forschungszentrums Jülich, Germany” at institute of energy and climate research IEK-5 Photovoltaics. The institute is equipped with solar simulator class A with AM 1.5 spectra as well as LED lighting used for Na ion battery charging (fabricated at IEK-9) with organic solar modules (fabricated at IEK-11) under reduced light power density.

2.1. Material used

2.1.1. Organic Solar Modules

Sample of organic photovoltaic modules used in this test has been supplied by IEK-11 Forschungszentrums Julich. The manufacturing method and the material are given in the article (Wagner, et al., 2023). Two small modules have been studied through their I-V characteristics. The modules are referred to as R2R081-42-1 and R2R081-42-2. Both modules have a surface area of 48cm^2 and contain 9 cells connected in series. The modules are encapsulated in a, flexible, semitransparent foil. The **Figure 2.1** shows the organic photovoltaic modules used in this work.

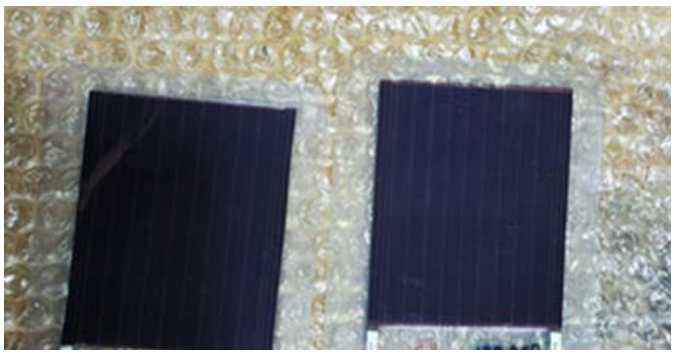

Figure 2.1: Organic photovoltaic modules.

2.1.2. Sodium (Na) ion battery

The sodium Na ion battery is provided by IEK-9. The capacity of the battery is 1.09 mAh, sits size is 1.13 cm^2. The set up of fabrication of this battery are as following.

- **Electrode sodium preparation:**

A4-sized of carbon nano felt (CNFs) with a thickness of 115 μm were obtained from Tortech Nano-Fibers (Ma'alot-Tarshiha, Israel). The CNFs were cleaned with concentrated hydrochloric acid and a mixture of ethanol/water (1: 1, v/v) several times before use in order to remove surface impurities. All other chemical reagents (of analytical grade) were purchased from Sigma-Aldrich and used as received.

A Sodium titanium phosphate oxide (NaTi–P–O) precursor solution was prepared by the dropwise addition of titanium (IV) isopropoxide (~0.05 mol) to ammonium hydroxide (30 mL) under constant vigorous stirring until a white gelatinous precipitate formed. The precipitate was washed with 500 mL deionized water to remove excess base and then dissolved in a 1 M solution of oxalic acid (200 mL) at 60°C under stirring until a transparent solution containing $H_2[TiO(C_2O_4)_2]$ was formed. Sodium acetate (5% stoichiometric excess) and a stoichiometric amount of ammonium dihydrogen phosphate were dissolved in water separately and then added slowly to the transparent solution. The final solution was transparent and slightly cloudy but does not settle after long periods.

- **Battery assembly method**

The electrochemical properties of the prepared electrodes were assessed in steel Swagelok cells with mylar liners. The assembly of all the test cells was carried out in an Ar-filled glovebox, where the concentrations of water and oxygen were kept at less than 0.1 ppm. The 12 mm diameter electrodes (1.13 cm^2) were cut directly from the prepared sheets, weighed, and then used without further modification. Metallic sodium foil was used as the counter electrode and pressed onto 11 mm nickel discs. Batteries were made with 1 M $NaPF_6$ in 2-methoxyethyl ether (DEGDME, or diglyme) electrolyte and glass fiber (Whatmann, GF1) separators. Electrolyte was dried with molecular sieve at least 1 day after preparation and kept with molecular sieve in a sealed bottle within the glove box thereafter to eliminate any trace water content, which was essential to ensure reproducible results. (Kin, et al., 2022).

2.2. Experimental procedures

2.2.1. Solar simulator measurements:

The solar simulator is an equipment used in this experiment to determine the PV characteristics of the organic solar module and to characterize quantum efficiency. The type of solar simulator used in this work is the Wacom Solar Simulator WXS-140S-Super. The schematic of the solar simulator is given on **Figure 2.2**.

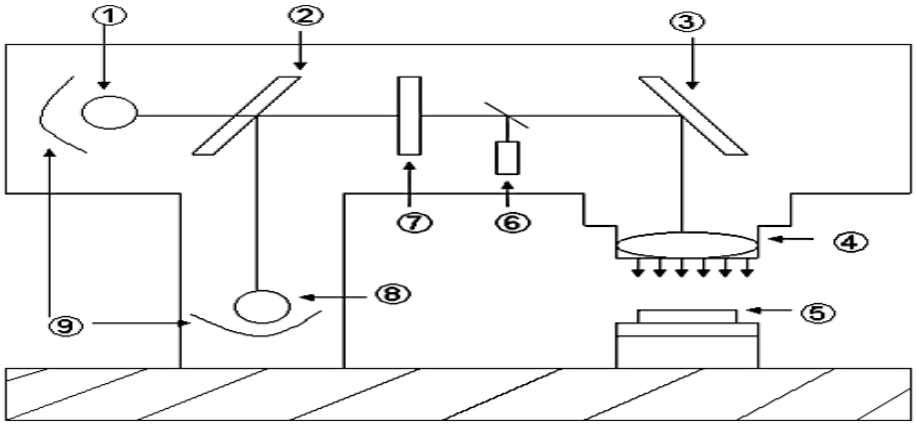

Figure 2.2 : Schematic structure of the solar simulator.

The radiation source is a halogen and a xenon lamp (1, 8). Both lamps are each fitted with an elliptical mirror (9), which parallels the light on a semi-transparent mirror (2). Light from the halogen lamp can pass through the mirror almost unhindered, while light from the xenon lamp is reflected. The two partial spectra are thus superimposed. The entire spectrum is irradiated to an integrator (7). Its task is to homogenize radiation intensity across the cross-section. A downstream beam splitter deflects a small portion of the light. This is used in a feedback loop (6) to fine-tune the xenon lamp. A large-area plane mirror (3) projects the calibrated spectrum onto the sample stage (5). If required, the luminous flux can be interrupted through an aperture (4). For temperature stabilization, the sample is sucked onto a copper block, enabling a constant sample temperature of 25°C to be achieved by means of an integrated electric heater with water cooling. The spectrum generated by the solar simulator corresponds approximately to the so-called AM1.5 spectrum (Zahren, et al.,2017) The I-V measurement is carried out in a closed laboratory using a solar simulator.

Characterization of Organic solar module underAM 1.5 spectrum (1 Sun):

The first experiment has been carried out to determine the parameters that characterize the OPV under one sun. I-V characteristic, with the photovoltaic (PV) parameter give information on the

performance of the photovoltaic module. The PV parameters are: P_{max}, V_{oc}, I_{sc}, n, and FF, I_{mpp}, V_{mpp} and the effect of R_s and R_{sh}.

In fact, I-V measurement requires a calibrated source that corresponds to real daylight and conditions that can be modified on demand to illuminate a photovoltaic panel. However, focusing on option two, we're going to determine the parameters that characterize the Organic solar module under one sun to standard test condition (STC) correspond to 100 mW/cm^2 and at temperature 25 ^{0}C. Before measuring the parameters of the solar module, the solar simulator needs to be calibrated, and the calibration is carried out on a photodiode cell or reference cell, which gives standard values so that the test can be carried out. Then, to determine I-V Characteristic of OPV, the solar module is placed under the solar simulator with similar radiation of sun with a temperature of 25 ^{0}C; positive and negative terminals solar module are connected to the voltmeter and ammeter measurement source, and a cooling system is set up under the sample to cool it.

The computer is equipped with the software for measuring current tension and other solar module parameters. Once these devices are switched on and the solar module is illuminated under solar simulator at 100 mW/cm^2, the other operations will be carried out using the software in the computer. This means that we put the necessary information on the software e.g., the surface area of our solar module, the number of cells, the AM1.5 measurement type, the maximum and minimum voltage, Voltage set, I compliance etc. **Figure 2.3** shows the equivalent single diode model for a solar device under illumination.

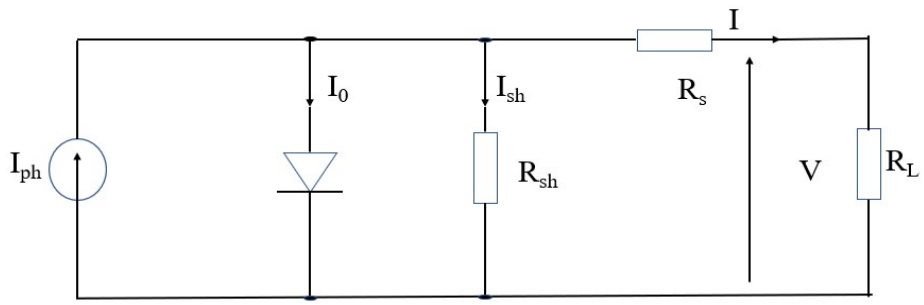

Figure 2.3: The equivalent single diode model for a solar cell under illumination.

With these five parameters, the equation for the solar cell's I-V curve is as follows:

$$I = I_{Ph} - I_0\left(e^{\frac{(V_{cell}+IR_{s,cell})}{nV_T}} - 1\right) - \frac{V_{cell} - IR_{s,cell}}{R_{sh,cell}}$$

V_T equal to kT/q where k is the Boltzmann constant J/K (1.381×10^{-23} J/K), q is the electronic charge (1.608×10^{-19} C), T is the absolute temperature in Kelvin, 298.15 K under STC, n Diode ideality factor. The equation parameters for a solar panel with Ns identical solar cells in series can be written following Equation (2.1) (Liu, et al., 2019) of single diode model for a solar cell under illumination.

$V = N_s \times V_{cell}$

$R_s = R_{s,\,cell}$

$R_{sh} = R_{Sh,\,cell}$

$$I = I_{Ph} - I_0\left(e^{\frac{q(V+IR_S)}{N_S nkT}} - 1\right) - \frac{V - IR_S}{R_{sh,cell}} \qquad \text{Eq (2.1)}$$

From **Figure 2.3** we can determine all the parameters (efficiency, fill factor, maximum power point) that characterized the solar device (cell or module) : . The shunt resistance and the series resistance can be determined from Ohm Law.

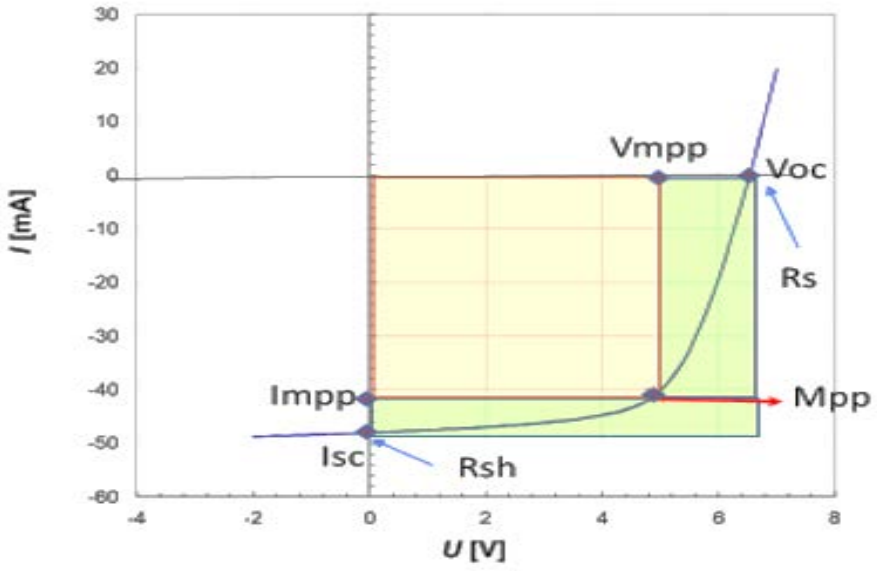

Figure 2.3 : I-V characteristic under one sun (AM1.5 irradiance).

- **Open-circuit voltage Voc:**

The open-circuit voltage, V_{oc}, is the maximum voltage available from a solar cell, and this occurs at zero current. The open-circuit voltage corresponds to the amount of forward bias on the solar cell due to the bias of the solar cell junction with the light-generated current, the Equation (2.2) expresses the formula of open-circuit voltage V_{oc}.

$$\mathbf{Voc} = \frac{\boldsymbol{nkT}}{\boldsymbol{q}} \boldsymbol{ln}\left(\frac{\boldsymbol{I_L}}{\boldsymbol{I_0}} + \mathbf{1}\right). \qquad \text{Eq (2.2)}$$

n Diode ideality factor.

q is the electronic charge (1.608×10^{-19} C).

T is the absolute temperature in Kelvin, 298.15 K under STC.

k is the Boltzmann constant J/K (1.381×10^{-23} J/K).

I_L light generate current.

I_0 Dark Saturation current.

- **Short Circuit Current (I_{sc}):** The short-circuit current results from the generation and collection of light-generated carriers; The short-circuit current, I_{sc}, is measured in mA. The short circuit current I_{SC} is the short circuit current density J_{SC}, times the cell area. Equation (2.3) expresses the relation between I_{sc} and J_{sc} (PV education, 2023).

$$I_{sc} = J_{sc}\ (mA/)\times A(cm^2) \qquad \text{Eq (2.3)}$$

  - **Maximum power point MPP**: is the point where the cell produces maximums power, it is the maximum product of current times voltages. Equation (2.4) gives the expression of maximum power point.

$$P_{mpp} = I_{mpp} \times V_{mpp} \qquad \text{Eq (2.4)}$$

V_{mpp}: is the output voltage at maximum power point

I_{mpp}: is the output current at maximum power point.

  - **Fill factor:** is defined as the ratio of the maximum power from the solar cell to the product of V_{oc} and I_{sc}; is one of the most important parameters of the solar module, fill factor determines solar module quality. The fill factor is calculated as follows:

$$FF = \frac{P_{mpp}}{Isc \times Voc} = \frac{Impp \times Vmpp}{Isc \times Voc} \quad \text{Eq (2.5)}$$

- **Efficiency:** Efficiency is defined as the ratio of the solar cell output power to the input power of light arriving at the solar cell. The efficiency depends on the spectrum and intensity of the incident light and the temperature of the solar cell. Efficiency determines the performance of our organic module and allows us to compare it with the performance of other modules. Equation (2.6) expression for determination of efficiency.

  $\eta = \frac{Pout}{Pin}$; $P_{out} = Impp \times Vmpp = FF \times Voc \times Isc.$

  Incoming power P_{in} is defined as:

  $P_{in} = Area\ of\ solar\ cell\ \times Plightin$

$$\eta = \frac{Voc \times Isc \times}{Area(cm^2) \times Ein(mW/cm^2)} \times FF \quad \text{Eq (2.6)}$$

- **Shunt resistance:** The shunt (or parallel) resistance R_{sh} results from a macroscopic defect in the solar cell, such as a crack through the semiconductor layers or a current path along the edge of the solar cell.
- **Serie resistance:** The series resistance R_s results from the semiconductor materials of the p-n junction, the interface between the p-n junction and the metal terminals/contacts, and finally, the metal terminals/contacts themselves (Loo, 2016).

2.2.2. Activation and stability tests of Organic solar module

Stability testing involves assessing the long-term performance and durability of organic solar modules under a range of environmental conditions. The aim is to understand how the modules degrade over time and to identify any potential problems that could affect their efficiency and lifespan.

The first charging and tuning of organic solar modules are referred to as activation. To guarantee that modules run at their peak performance levels after manufacture, they might need to go through an activation process.

Stability and activation process carried out in this work consists of placing the solar module under AM 1.5 illumination for six hours, at the end of which its value remains stable for these hours. in the first hour which corresponds to the activation time.

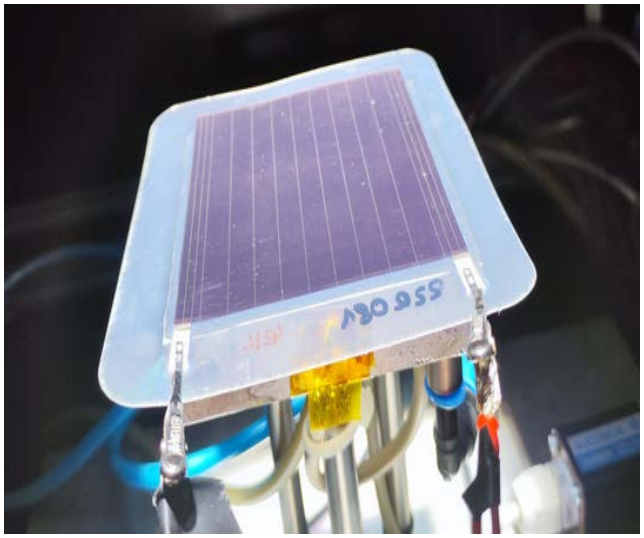

Figure 2.4: Photo of the stability and Activation of opv under one sun AM1.5.

2.2.3. Partial Shading test for organic solar module:

The modules used in this work in variety of illumination scenario produce current which exceeds current limits of the small battery cell available for the charging experiment. To match output current of the PV modules to the battery cell, the modules are partially shaded preserving equal shading of all solar cells of the module. Different degrees of shading have been tested for the organic solar module of 9 cells and a surface of 48 cm^2, from 10% to 90%.

We have chosen two samples of solar modules with similar I-V characteristics for this test. **Figure 2.5** shows the shading test set up.

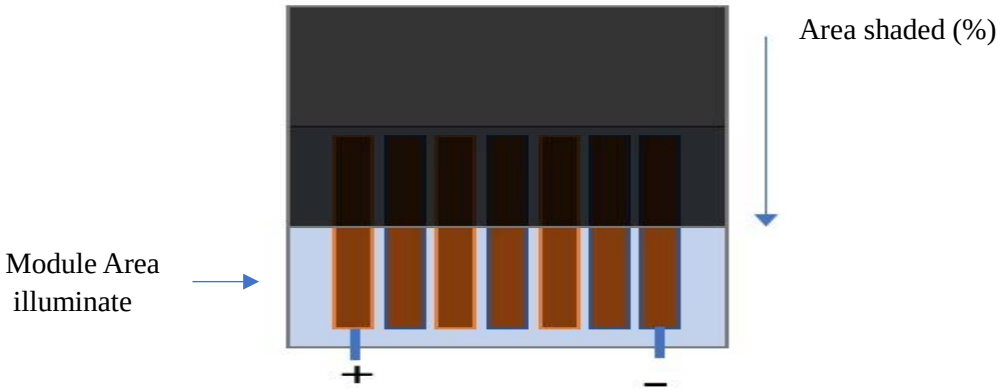

Figure 2.5 : Partial shading test set up.

- The surface of the solar module is illuminated during the shading test at different percentages under one sun according to the Equation (2.7) below.

$$Area_{ill}(cm^2) = \frac{Surface\ total\ Area\ (cm^2) \times (100 - Number\ of\ percentage\ of\ surface\ shade)}{100}$$ Eq (2.7)

- The distance determination corresponding to the different percentage on the solar module **(Table 2.1).**

$$Length = Length\ of\ module\ solar \times Number\ of\ shade\ [\%]$$ Eq (2.8)

Table 2.1: Values of module area illuminated and the length of shading (%)

Shade [%]	Module Area illuminate cm^2	Length cm
0	48	0
10	43.2	0.8
20	38.4	1.6
30	33.6	2.4
40	28.8	3.2
50	24	4
60	19.2	4.8
70	14.4	5.6
80	9.6	6.4
90	4.8	7.2
100	0	8

The second step of the experiment is to measure I-V characteristics at each degree of shadowing. To do this, the solar module is partially covered with a flat metallic plate, starting from the case without shade, and then for different shading degrees from 10 to 90%. At the end of the experience, the efficiency of the solar module is determined for each shading percentage of radiation of 100 mW/cm^2 (Equation (2.9)).

The determination of the efficiency of shading is as follow:

$$\text{Efficiency } \eta\ (\%), Area_{ill} = \frac{Voc \times Isc}{Area_{ill}(cm^2) \times Ein(mW/cm^2)} \times FF$$ Eq (2.9)

2.2.4. Neutral-density filters:

Neutral-density filters are used to reduce the light intensity uniformly across the AM 1.5 (1 Sun) or LED spectrum. **Figure 2.6** shows the different filters used to reduce light intensity under 1 Sun or LED illumination. These filters are made of glass with a black coating on the layer, they are graded from the finest transparency to high transparency.

Five neutral-density filters, are used, we started to measure the solar module without filter which corresponds to the normal measurement value under one sun. After, we continue with the weakest colors of black transparency and strong transparency, then some filters are also

combined to observe different irradiance effects on the solar module. The filters are placed on top of the solar module and exposed to illumination under simulated sunlight. For this experiment the module efficiency is determined by the formula including effect of attenuation with filters Equation (2.10).

$$\eta = \frac{\boldsymbol{Voc}\times \mathrm{Isc}}{\boldsymbol{Area}\times\boldsymbol{Fx}\times\boldsymbol{Ein}} \times \mathrm{FF} \qquad \text{Eq (2.10)}$$

Area: is the total area of the module, 48 cm^2.

F_x: value of attenuation.

FF: Fill factor.

E_{in}: is the energy input of sun simulator 100 mW/cm^2.

Figure 2.7: Photo of Filters uses under one Sun AM1.5.

2.2.5. Photovoltaic Characterization under LED irradiance of organic photovoltaic module:

The device used to characterize the organic photovoltaic module OPV under LED illumination is a so-called LED solar simulator. LED equipment is based on Osram 5.5 W PAR16 LED spotlight (4000k), 20cm from the module aperture. LED simulator is equipped with a white LED lamp and connected to the measurement source and computer. These simulators use white LED and their spectra is different than the AM1.5 spectral of natural sun light because the spectrum of LED is narrower and weaker than the spectrum of natural sun light.

For LED test measurement solar module is placed under white LED illumination. Unlike irradiance outdoors it is typical for the indoor lighting to be characterized with photometric

illuminance related to the human eye light perception. The illuminance is expressed in Lux (lux). Illuminance does not describe the whole spectrum of light indoors and is used here for orientation and link to the indoor illumination standards. In this test the measurement procedure is similar to that of solar simulator with AM1.5 spectrum (1 Sun) but the difference is for LED tests, the intensity of the light depends on the voltage set and the; light LED is artificial light. The **Table 2.2** below indicates that each voltage corresponds to its irradiance level and its value Lux of LED. **Figure 2.8** shows the LED measurement set up. The same mathematical formula is used to determine the electrical parameters of the solar module under LED irradiance as for the AM1.5, but for the LED the irradiance energy input depends on the voltage set.

Table 2.2: The voltage set and irradiance LED and Lux values

Vset (V)	**E_{in} (mW/cm^2)**	**Lux (lx)**
30	0.035	103
30.1	0.046	140
30.2	0.062	189
30.3	0.081	249
30.4	0.107	330
30.5	0.14	433
30.6	0.181	560
30.7	0.237	711
30.8	0.304	904
30.9	0.383	1125
31	0.494	1385
32	1.936	5980
33	4.04	12660
34	6.216	18850
35	8.491	20180

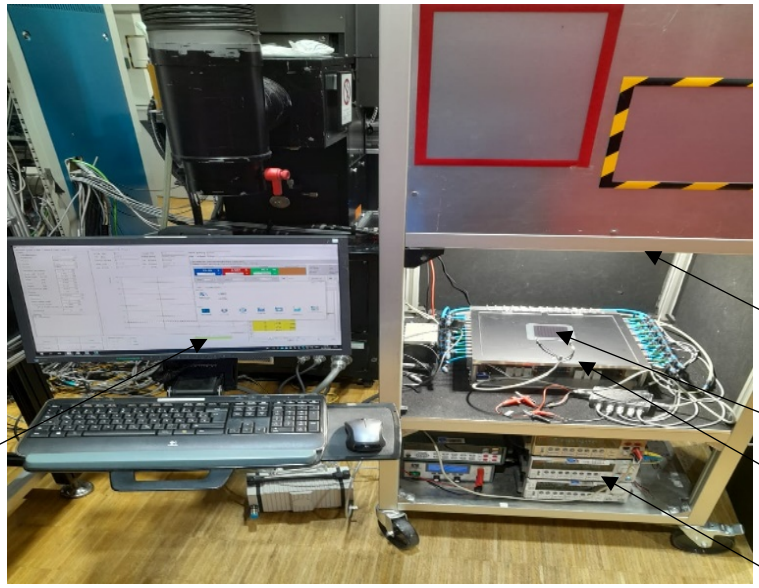

Figure 2.8: LED measurement Set up.

2.2.6. Quantum Efficiency Characterization:

Quantum efficiency is the basis for understanding short-circuit current, provides information on the optical properties of the cell, and (limited) information on electronic properties.

The external quantum efficiency EQE is defined as the number of electrons per photon impinging on the solar cell. The EQE is a spectral quantity depending on the wavelength λ. **Figure 2.9** illustrates quantum efficiency measurement set up.

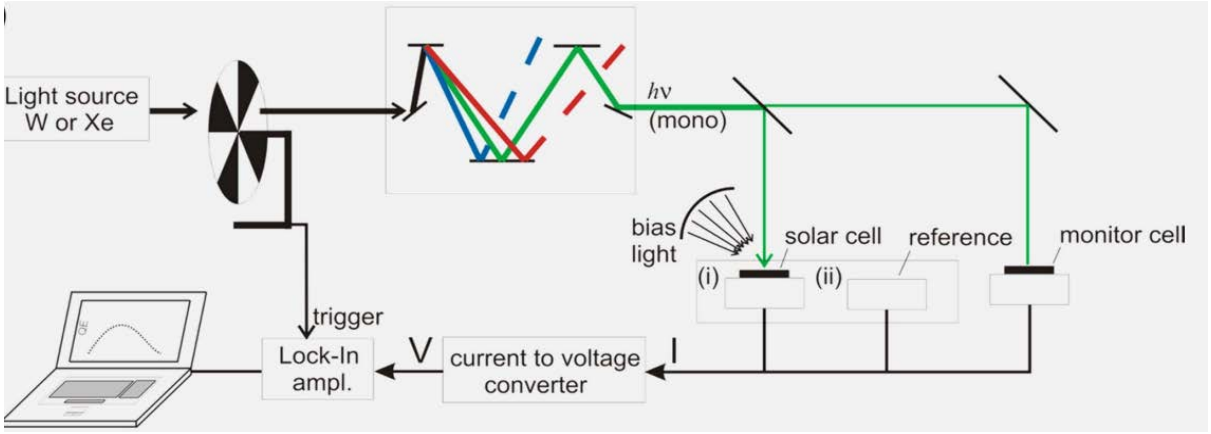

Figure 2.9 : Quantum efficiency Measurement set up (Rau, 2023).

The measuring device comprises a light source, optical components for beam conditioning, a device under test (e.g., a photodiode or solar cell) and a detector for measuring the output signal. Before carrying out QE measurements, it is essential to calibrate the intensity of the

light source and the detection system in order to obtain accurate and reliable results. The device under one sun is illuminated by a known, stable light source. The light source may be a monochromatic laser, a broadband light source combined with filters, or a specific wavelength LED, depending on the application and wavelength range concerned. The device's output signal is detected and measured using appropriate instruments.

The photocurrent generated is usually measured using a current meter or lock-in amplifier. To calculate the EQE, a reference measurement is made using a known standard whose quantum efficiency is well characterized. This reference measurement is used to normalize the measurement and correct for any configuration-dependent factors. The formulas for calculating the efficiency of the two quantum's are as follows:

- External quantum efficiency: Equation (2.11).

$$EQE\ (\lambda) = \frac{hc \times Jsc(\lambda)}{q(\lambda) \times P_{ill}(\lambda)} \qquad \text{Eq (2.11)}$$

We measure the short-circuit current J_{SC} as a function of the incident illumination power (P_{ill}) at different λ.

h : Planck's constant 6.6210^{-34} Js

C : Speed of light 2.99 m/s

q : Elementary charge 1.610^{-19} C

λ : Wavelength of light in nm

The internal quantum efficiency IQE is the EQE corrected for the spectral reflectance R(λ) Internal quantum efficiency: Equation (2.12).

$$IQE = \frac{EQE(\lambda)}{1 - R(\lambda)} \qquad \text{Eq (2.12)}$$

The performance of any solar cell or photodiode is largely governed by the incident photon to converted electron efficiency, that is, the externally measured ratio of the number of collected charges to the number of incident photons often referred to as the external quantum efficiency (EQE) (Armin, et al., 2014).

2.2.7. Battery charging and discharging set up under LED:

To test organic modules charging batteries indoors under LED lighting, the photovoltaic module is placed under the indoor LED simulator, and the negative and positive terminals are connected to the source measurement for the measurement of current and voltage. The battery

is directly coupled to PV; 2 kΩ of resistance is applied for discharging the battery. The information is collected by the data acquisition system.

Once the battery is charged by photovoltaic device and discharged by 2 kΩ, we determine the coupling factor, the working point, and the overall efficiency of the battery. The following tables show the different charging and discharging times and the energy stored in the battery.

Table 2.3: Parameter of battery characteristic Module 42-1 under LED

Lux (lx)	LED Voltage (V)	Pin (W/m^2)	Charging time (min)	Charging current (mA)	Stored charge (mAh)	Discharge current (mA)	Discharge time (min)	Discharge time (s)
433	30.5	1.4	7	0.009	0.00105	1	0.063	3.78
560	30.6	1.81	7	0.035	0.00408	1	0.245	14.7
711	30.7	2.37	7	0.068	0.00793	1	0.476	28.56
904	30.8	3.04	7	0.111	0.01295	1	0.777	46.62
1125	30.9	3.83	7	0.16	0.01866	1	1.12	67.2
1385	31	4.94	7	0.217	0.02531	1	1.519	91.14
5980	32	19.36	7	1.459	0.17021	1	10.213	612.78
12660	33	40.4	7	2.85	0.3325	1	19.95	1197

Table2.4: Parameter of battery characteristic for Module 42-1. Under LED

Lux (lx)	LED Voltage (V)	Pin (W/m^2)	Charging time (min)	Charging current(mA)	Stored charge (mAh)	Discharge current (mA)	Discharge time (min)	Discharge time (s)
433	30.5	1.4	7	0.028	0.00326	1	0.196	11.76
560	30.6	1.81	7	0.055	0.00641	1	0.385	23.1
711	30.7	2.37	7	0.088	0.01026	1	0.616	36.96
904	30.8	3.04	7	0.128	0.01493	1	0.896	53.76
1125	30.9	3.83	7	0.172	0.02006	1	1.204	72.24
1385	31	4.94	7	0.23	0.02683	1	1.61	96.6
5980	32	19.36	7	1.42	0.16566	1	9.94	596.4
12660	33	40.4	7	2.8	0.3266	1	19.6	1176

Battery charging time was set to 7 minutes in the experiment. To determine the discharge time for complete utilization of charge. the charge stored in the battery in mAh has been multiplied by the discharging current of 1 mA and so the battery discharge time is determined as

$$\text{Stored charge (mAh)} = \frac{\text{Charging current (mA)} \times \text{charging times(minutes)}}{60} \qquad \text{Eq (2.13)}$$

$$\text{Discharge times (minutes)} = \frac{\text{Stored charge (mAh)}}{\text{Dichargind current(mA)}\times 60} \qquad \text{Eq (2.14)}$$

The discharge time in second = Dicharge times (minutes) × 60

After this, the various parameters for battery performance under LED are determined: Power working point, PV charging efficiency, coupling factor.

$$\text{Coupling factor} = \frac{\text{Power working point}}{\text{Power maxium point}} = \frac{\text{Iwp}\times\text{Vwp}}{\text{Impp}\times\text{Vmpp}} \qquad \text{Eq (2.15)}$$

P_{wp} refers to the power at the working point of the coupled system with respect to the solar module at a specific irradiance. The working point (Wp) during charging is determined by the intersection of the I-V characteristics of the photovoltaic module with the battery I-V characteristics (Kin, et al., 2022). Iwp is the current at working point; Vwp the voltage at working point during the battery the charging.

$$\text{PV charging efficiency} = \frac{\text{Power working point}}{\text{Power LED}} \qquad \text{Eq (2.16)}$$

$$\text{Overall efficiency} = \frac{\text{Energy dicharge of battery}}{\text{Energy of LED}} = \frac{\int_{td,start}^{td,end} P_{bd}\,dt_d}{\int_{tc,start}^{tc,end} P_{LED}\,dt_c} \qquad \text{Eq (2.17)}$$

P_{bd} is the power of battery in discharge and P_{LED}: power of LED in charging. The t_d end discharge time at end. $t_{d,\,start}$ discharge time at beginning.t_c, end time of charging at end; $t_{c,\,start}$ time of charging at start.

The **Figure 2.10** depicted the battery and PV coupling for charging and discharging condition.

a) Charge off and Discharge off , the solar module is in short circuit condition.
b) Charge is on , Discharge off , solar module Voltage equal to battery voltage, battery is in Charging.
c) Charge on and the Dicharge on, the solar module is open-circuit voltage battery is in discharging.
d) Charge off , Discharge on solar module is in short circuit current condition and Battery is dicharging.

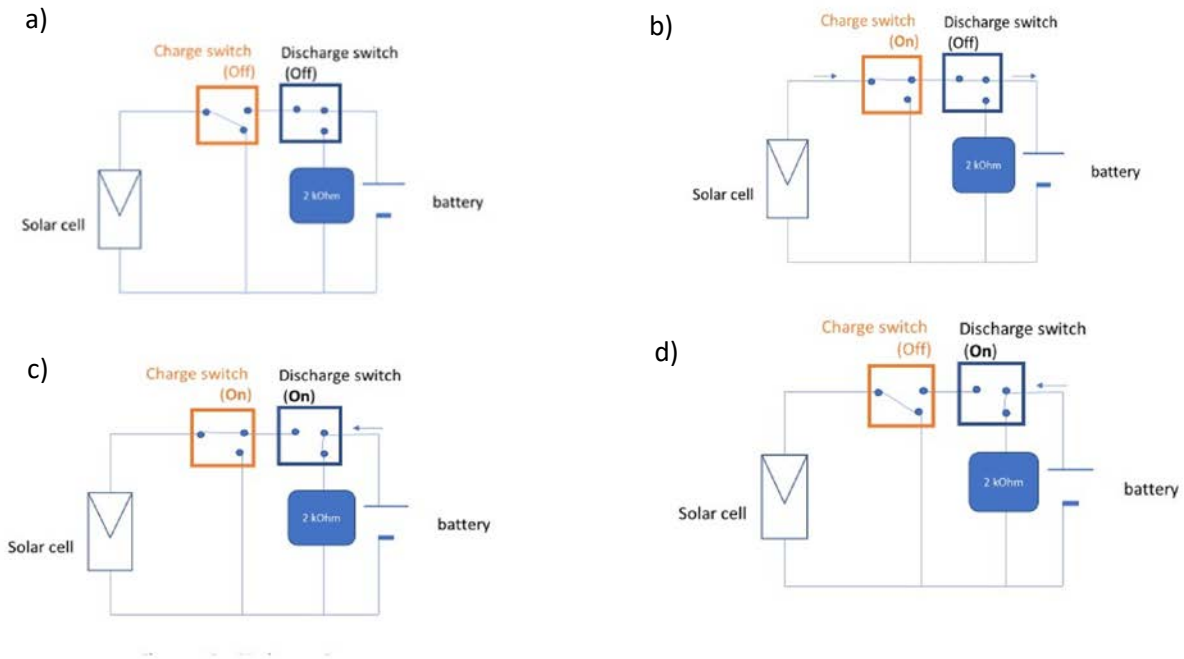

Figure 2.10: Battery charging and discharging couple with solar module systems.

2.2.8. Software used:

Origin pro2 018 software is used to plot data.This sofware is to used realize the different curves and also to analyze the obtained data.

CHAPITER 3: RESULTS AND DISCUSSION

3.1 Characterization of Organic solar modules under AM 1.5 irradiance:

The **Table 3.1** shows the different Photovoltaic (PV) parameters of organic photovoltaic (OPV) modules obtained from I-V measurement under one sun AM1.5 irradiance (1 Sun). The efficiency of organic solar module, their fill factor, the short-circuit current, the open-circuit voltage and the shunt and series resistance are shown in **Table 3.1**. The solar conversion efficiency of OPV module is 4.2%, the fill factor reaches 64.2%. The fill factor value (FF) explains less shunt resistance and series under one sun AM1.5, above of 40% as a fill factor, this will explain a manufacturing defect in the module and result in an increase in shunt resistance which is the opposite in this experiment. At 25% of fill factor, considered a bad fill factor value, there is sufficient current loss in the module when exposed to natural light or to under one sun AM1.5 **Figure 3.1** shows the current-voltage (I-V) characteristic of the OPV module understudied in this work. The I-V measurement was performed under AM1.5 irradiance (1 Sun).

Table 3.1: PV parameter of OPV module measured under AM1.5 irradiances

Parameters	Values
η [%] :	4.2
FF [%] :	64.2
P_{mpp} [mW] :	201.1
V_{mpp} [V] :	4.901
I_{mpp} [mA] :	41.0
V_{OC} [V] :	6.528
I_{SC} [mA] :	48.0
J_{SC} [mA/cm^2] :	1.0
A [cm^2] :	48
$R_{S\text{-}Voc}$ [Ω] :	25.4
$R_{SH\text{-}Isc}$ [Ω] :	2275.5

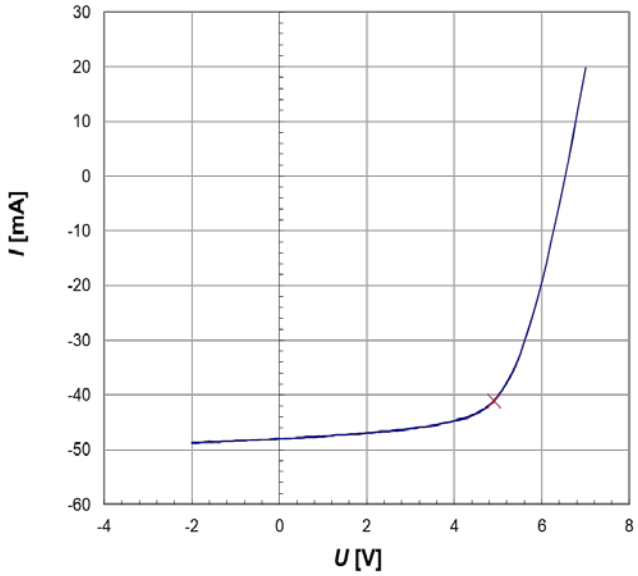

Figure 3.1: I-V curve OPV module.

3.2. Activation of OPV solar modules and stability

The various graphs show the results of OPV activation and stability under an AM1.5 sun. As shown in **Figure 3.2**, The different electrical parameters of the OPV are plotted as a function of time activation. The first hour corresponds to the activation of the module which begins with an efficiency of 3.7%; and for 7 hours of lighting under one sun AM1.5, **in Figure 3.2 (a)**, the efficiency is 4.2%. In **Figure 3.2 (b)** the fill factor values are 64.3%. in **Figure 3.2 (c)**, open-circuit voltage is 6.7 V and finally in **Figure 3.2 (d)**, the short-circuit current which decreases with time to 48 mA. OPV efficiency under AM1.5 for 7 hours gives good stability i.e., normal operation of the module. This stability test allows to know the effectiveness of the OPV solar module during a long period of operation.

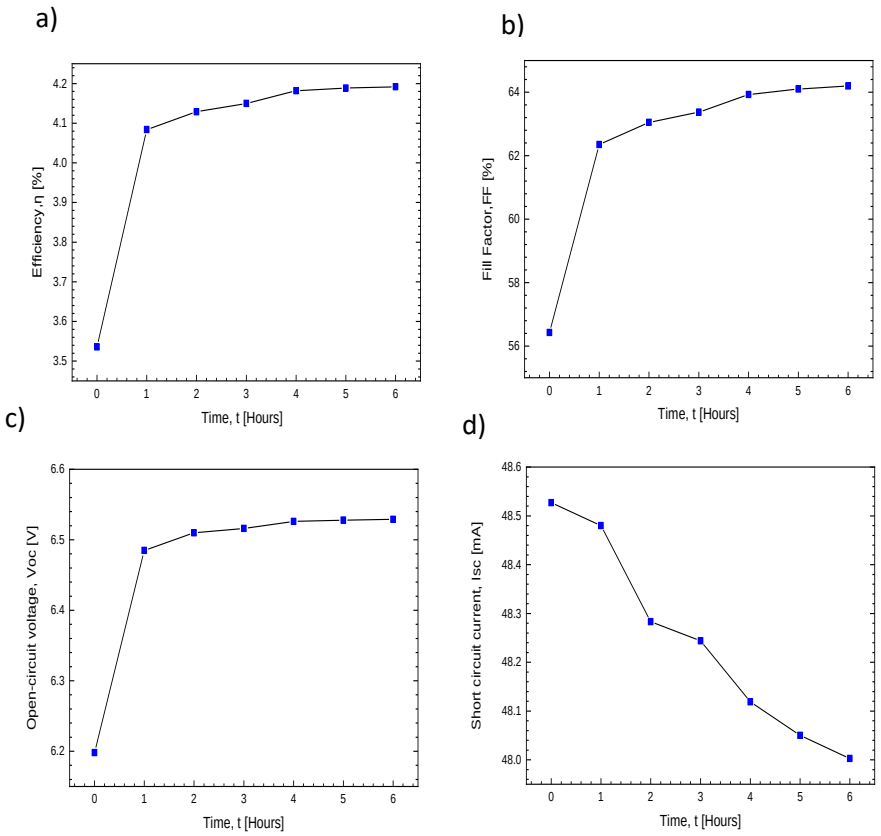

Figure 3.2: Graphs activation and stability Versus est time (Hours).

3.3. Partial Shading of OPV solar modules

In directly coupled PV-Battery device the I-V characteristic of PV and battery has to be similar in order to achieve good power transfer form PV to battery and finally charge the battery. In our case Na-ion battery has low capacity of 1.09 mAh and PV module has much higher short circuit current of 48 mA.

We have to reduce the short-circuit current of the PV module via partial shading to see if battery charging under AM 1.5 is possible. The **Figure 3.3** represents the PV parameters of the module against to the value of shadings estimated in %.

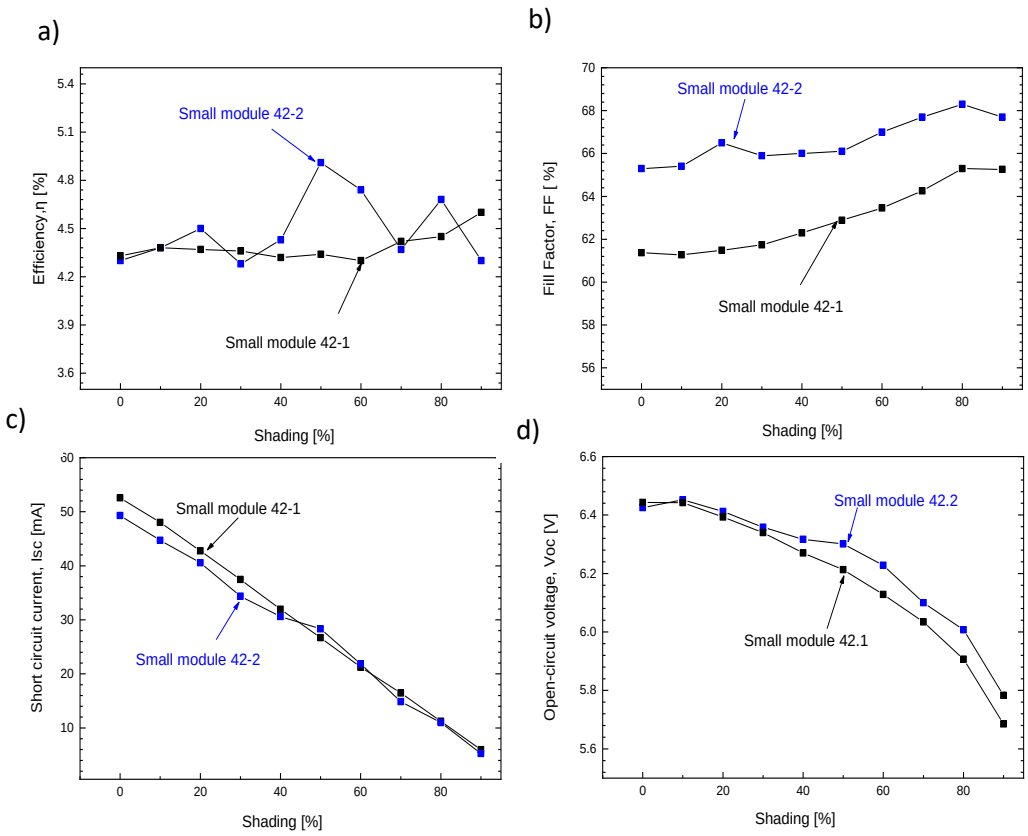

Figure 3.3: PV parameters of OPV solar modules versus partial shading in (%).

3.4. Effect of reduced AM 1.5 irradiance on the I-V characteristics of OPV modules

The **Figure 3.4** shows the normalized I-V characteristics of two OPV modules studied under reduced AM 1.5 irradiance by using various neutral density filters.

The shape of I-V curve changes with decreasing irradiance via attenuated AM 1.5 spectrum with neutral density filters. At a low irradiance, the I-V curve almost becomes a straight line which results in reduced efficiency and poor fill factor, and insufficient light absorption by the modulated cells to generate current. Black arrow shows direction of increase in irradiance spectrum under one sun. With Strong dependence the Shunt resistance reduce the Fill factor.

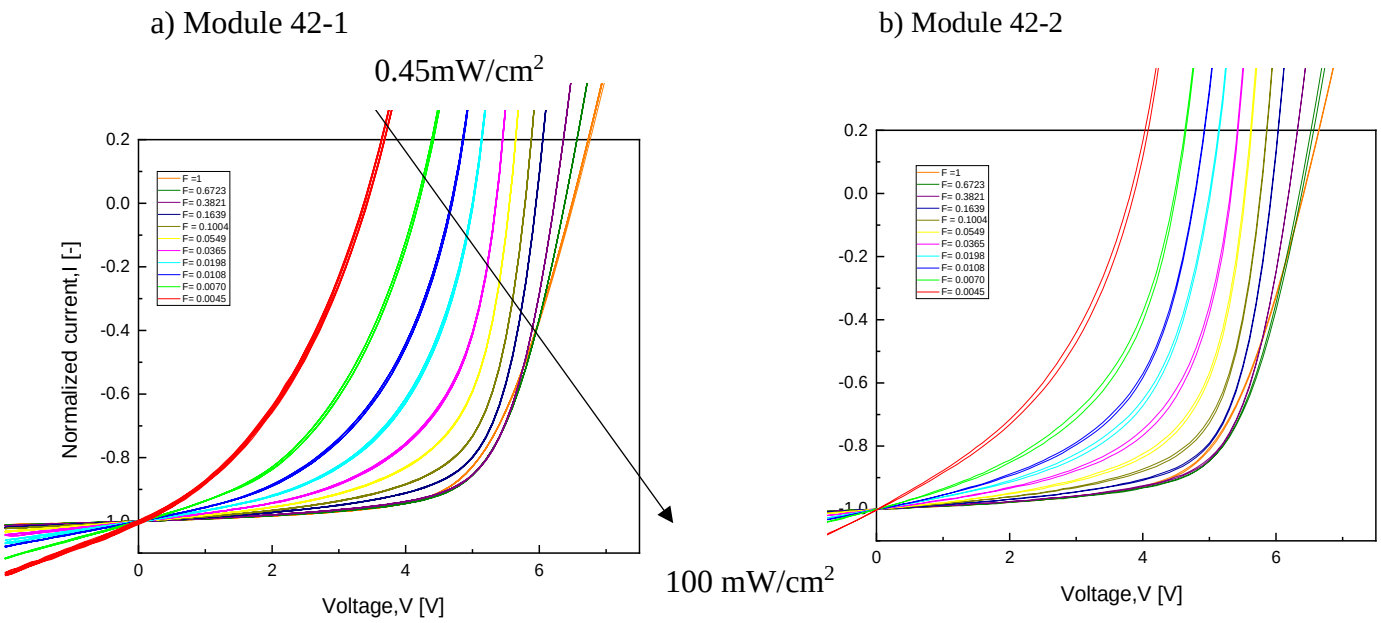

Figure 3.4 : Normalized current (-) Versus Voltage(V) curves for 2 OPV modules investigated under reused AM 1.5 irradiance.

3.5. External quantum efficiency of OPV modules

The external quantum efficiency (EQE) was measured for both OPV modules showing similar IV characteristics are plotted in the **Figure 3.5**. The spectrum of EQE gives information about the wavelength of light that the OPV solar module can efficiently convert into electricity. The number of charge carriers' electrons collected by the device to the number of incident photons correspond to 41% at wavelength of 500 nm in this organic photovoltaic module. Compared this value to the EQE value with the review (Kin, et al., 2022) which is 83% at 500nm, shows that the organic module used in this work needs to be further improved.

a) Small module 42-1

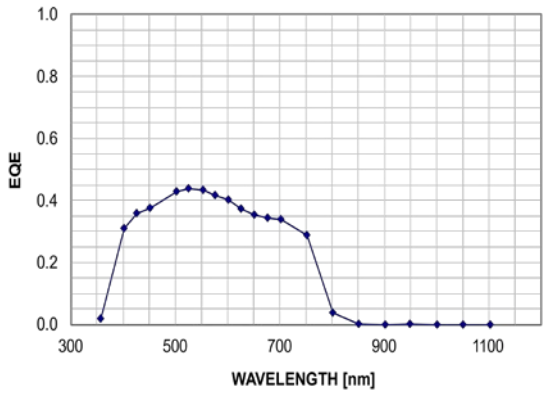

b) Small module 42-2

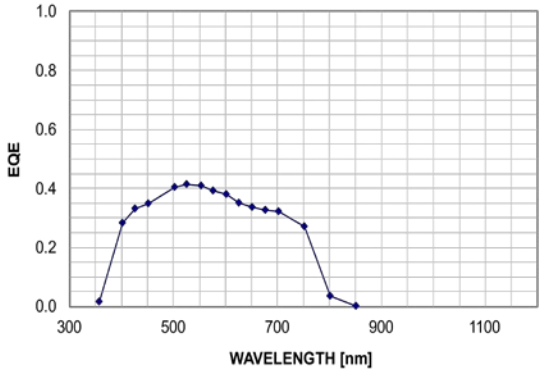

Figure 3.5: External Quantum efficiency of the OPV modules.

3.6. Influence of the reduced AM 1.5 and LED light power density on the PV parameters of OPV modules.

The photovoltaic parameters of a OPV modules obtained by reducing the AM 1.5 or LED light power density using the neutral density filters are compared in **Figure 3.6**. On the left is the first module, where the values of the PV parameters V_{oc}, V_{mpp}, FF, Ƞ for AM1.5 irradiance and LED irradiance of the OPV module are plotted as a function of intensity in mW/cm^2. On the right, we have the results for the second module.

The value between 300-500 lux corresponding to a LED light power density of 0.107-0.284 mW/cm^2 are suitable for indoor applications. In the region 300-500 Lux of LED spectrum, the V_{oc} value of 1.98 - 2.73 V are measured; and a V_{mpp} of 1.1- 1.59 V, the FF is between 37.25-37.16 % and the $Ƞ_{LED}$ is 1.11- 1.68 %. For an intensity of less than 0.494 mw/cm^2 the organic solar parameters are null under AM1.5 in the case of first module 42-1.

For the second module we have a V_{oc} values of 2.40-2.89 V, V_{mpp} 1.36-1.67V, FF 31.62-33.58 %, $Ƞ_{LED}$ is 1.39 - 1.51%.

The **Figure 3.7** shows series and shunt resistance for the both OPV modules under LED irradiance 300-500 Lux and AM1.5 irradiance. Strong dependence on irradiance, the performance heavily affected by R_{sh}.

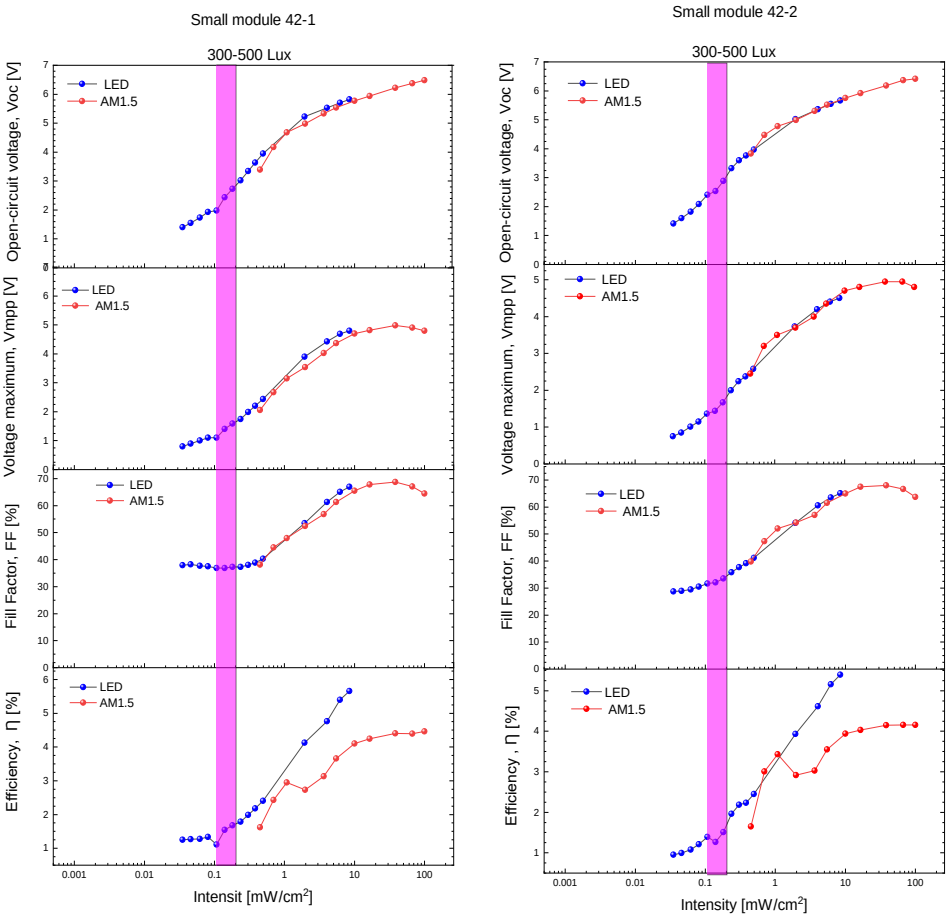

Figure 3.6: Graph's comparisons of PV parameters for two OPV modules with similar I-V caharacteristcs as a function of LED and AM 1.5 vs light power density.

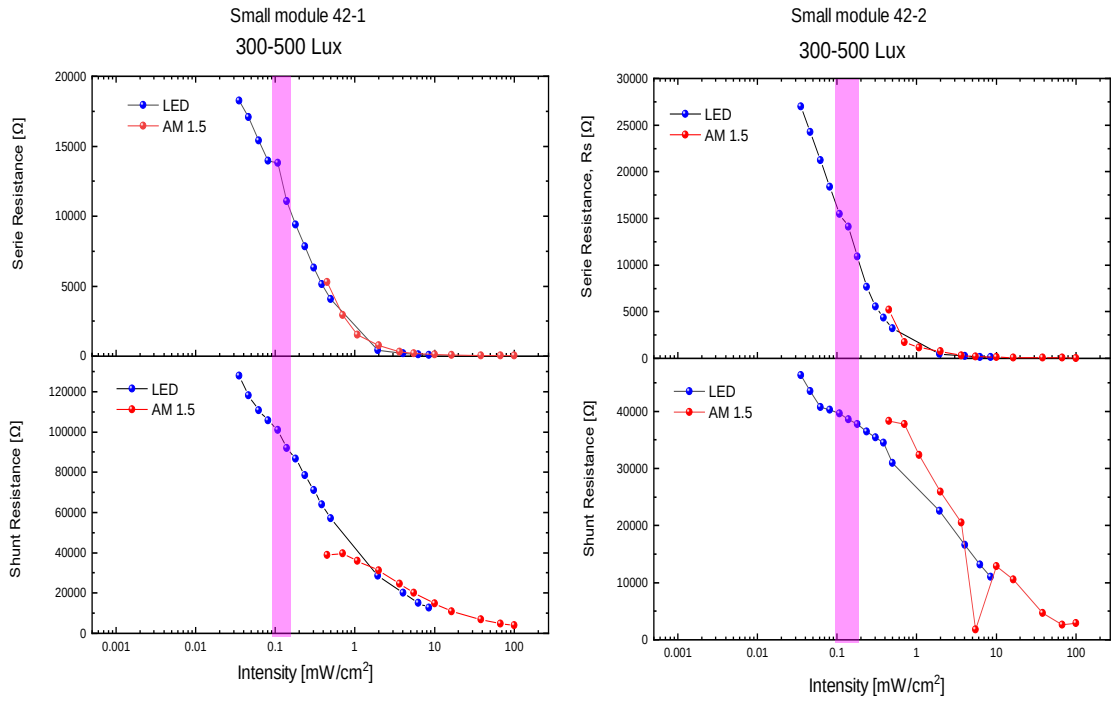

Figure 3.7: Graphs comparisons Series and Shunt resistance of LED and AM 1.5 vs light power density.

3.7. Battery charging under LED Light

The results of battery charging under LED irradiance via directly coupled OPV modules are shown in **Figure 3.8**. Both OPV modules show similar charging behavior. The target region for indoor application is 300-500 Lux of LED lightning and charging of the battery.

For the first module, the maximum efficiency of organic photovoltaic η_{OPV} reached is 4.89% with a current density J_{sc} of 0.057 mA/cm^2, the efficiency PV-to battery $\eta_{pv\text{-}to\text{-}battery}$ is 3.24%, The overall-efficiency $\eta_{overall}$ is 3.07%. The different voltages values, open-circuit voltages V_{oc}, maximum voltages point Vmpp, Voltage at working point V_{wp}. The V_{oc} is 5.55 volt, V_{wp} 2.20V V_{mpp} 4.50V. The fill factor during this PV coupled to battery is 60.9% for the first module.

For the second module the η_{OPV} is 4.68% with current density J_{sc} of 0.051 mA/cm^2. The $\eta_{pv\text{-}to\text{-}battery}$ 3.15%, $\eta_{overall}$ 3.01%. volage is “Voc 5.52V, Vwp 2.19V, Vmpp 4.30, V” their fill factor is 60.25%. The coupling factor in these range of 300-500 Lux for the first module is 0.67% and for second is 0.66% is better for this type of module.

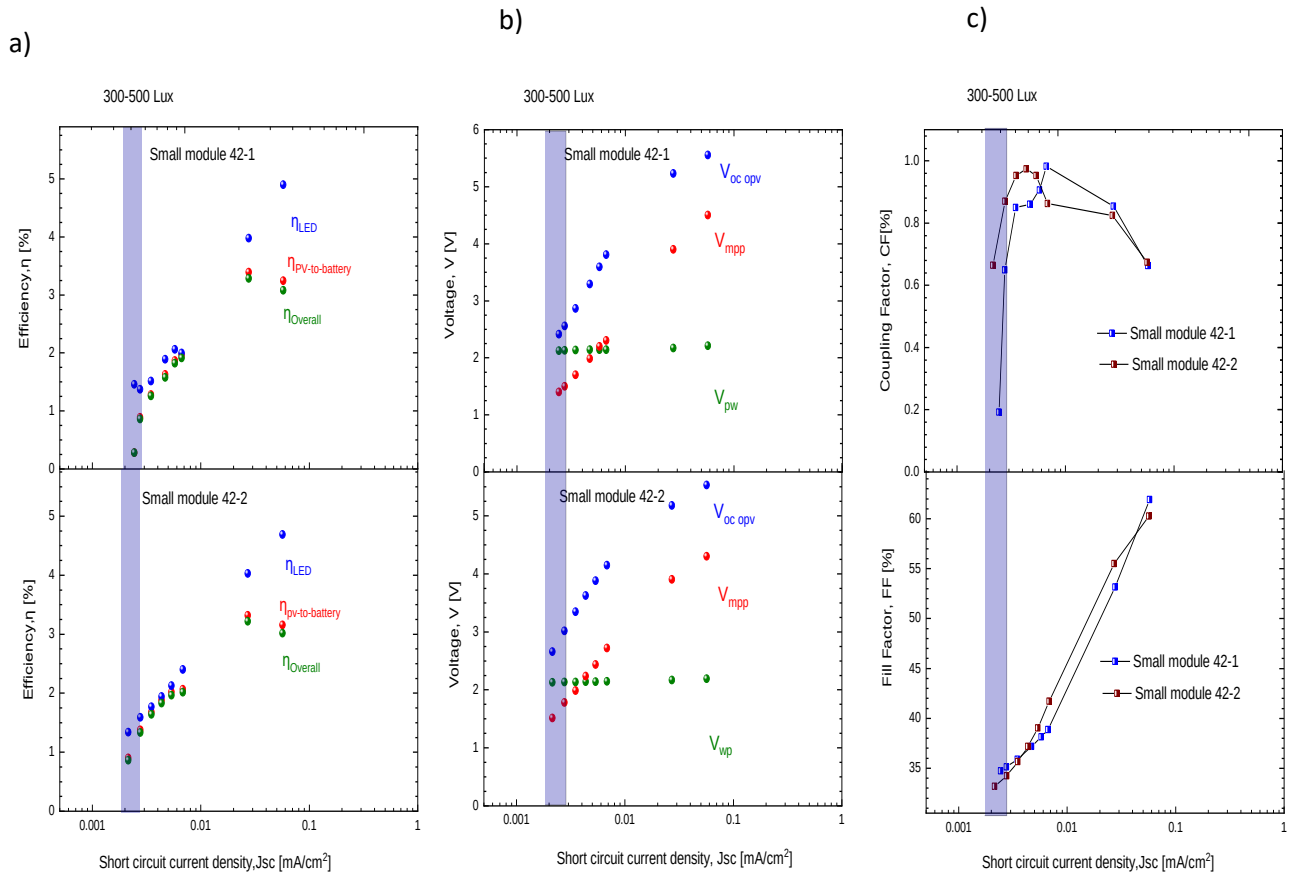

Figure 3.8: Results of the charging expreiment. (a) OPV efficiency, battery charging efficiency, and overall efficiency of the PV-battery combination; (b) open circuit, maximum power and Operating voltages of the OPV modules during charging; (c) PV-battery couplin factor, Fill Factor.

CONCLUSION AND PERSPECTIVES

In conclusion Indoor LED battery charging with organic photovoltaic represents an innovative and sustainable approach to harnessing energy from indoor lighting sources.

This technology can offer several advantages, including energy efficiency, flexibility and the ability to power low-power devices and systems in environments where traditional energy sources may be limited. Advances in materials and technology continue to improve the efficiency and reliability of organic photovoltaic. The potential applications for this technology are set to grow, making it an exciting area for development in the field of renewable energy and energy storage.

In this work, performance of Organic photovoltaic (OPV) in indoor application has been studied. OPV shows strong dependance on irradiance (AM1.5 and LED) mostly due the shunt resistance. Despite low FF of 60.9% succeful charging of sodium ion Battery has been demonstrated With The efficiency of the organic photovoltaic in 4.98% and PV-to battery efficiency of 3.25%, overall efficiency found is 3.07% under an LED light power density 300-500 lux.

In perspectives: Organic photovoltaic (OPV) needs to be optimized for higher Rsh to be comparative under indoor condition. Also, integration options for OPV modules and Na-ion batteries need to be explored.

REFERENCES

Zahren, C. & Gerber, A., 2017. Experiment Solar Cell I. *at Forschungszentrum Jülich Institute for Energy- and Climate Research IEK 5 - Photovoltaik,* Band 1.5.

Agbo, S. N., Merdzhanova, T., Rau, U. & Astakhov, O., 2017. Illumination intensity and spectrum-dependent performance of thin-film silicon single and multijunction solar cells. *Solar Energy Materials and Solar Cells,* Band 159, pp. 427-434.

Armin, A. et al., 2014. Quantum Efficiency of Organic Solar Cells: Electro-Optical Cavity Considerations. *ACS Photonics,* 1(3), pp. 173-181.

Astakhov, O., Merdzhanova, T., Kin, L.-C. & Rau, U., 2020. From room to roof: How feasible is direct coupling of solar-battery power unit under variable irradiance?. *Solar Energy,* Band 206, pp. 732-740.

Ben, M. & Veelaert, P., 2014. A Proposal for Typical Artificial Light Sources for the Characterization of Indoor Photovoltaic Applications. *Energies,* 7(3), pp. 1500-1516.

Bodnár, I., Koós, D., Iski, P. & Skribanek, Á., 2020. Design and Construction of a Sun Simulator for Laboratory Testing of Solar Cells. *Acta Polytechnica Hungarica,* 17(3), pp. 165-184.

Chime, U. et al., 2022. How Thin Practical Silicon Heterojunction Solar Cells Could Be? Experimental Study under 1 Sun and under Indoor Illumination. 6(1), p. 2100594.

Cui, Y., Hong, L. & Hou, J., 2020. Organic Photovoltaic Cells for Indoor Applications: Opportunities and Challenges. *ACS Applied Materials & Interfaces,* 12(45), pp. 38815-38828.

Cutting, C. L., Bag, M. & Venkataraman, D., 2016. Indoor light recycling: a new home for organic photovoltaics. *Journal of Materials Chemistry C,* 4(43), pp. 10367-10370.

Dennler, G. et al., 2007. A self-rechargeable and flexible polymer solar battery. *Solar Energy,* 81(8), pp. 947-957.

Esen, V., Sağlam, Ş. & Oral, B., 2017. Light sources of solar simulators for photovoltaic devices: A review. *Renewable and Sustainable Energy Reviews,* Band 77, pp. 1240-1250.

Ge, Z. et al., 2021. Recent progress of organic photovoltaics for indoor energy harvesting. *Nano Energy,* Band 82, p. 105770.

Goo, J. S., Shin, S.-C., You, Y.-J. & Shim, J. W., 2018. Polymer surface modification to optimize inverted organic photovoltaic devices under indoor light conditions. *Solar Energy Materials and Solar Cells,* Band 184, pp. 31-37.

Hoefler, S. F. et al., 2020. New Solar Cell–Battery Hybrid Energy System: Integrating Organic Photovoltaics with Li-Ion and Na-Ion Technologies. *ACS Sustainable Chemistry & Engineering,* 8(51), pp. 19155-19168.

Jahandar, M., Kim, S. & Lim, D. C., 2021. Indoor Organic Photovoltaics for Self-Sustaining IoT Devices: Progress, Challenges and Practicalization. *ChemSusChem,* 14(17), pp. 3449-3474.

Jo, J. et al., 2009. Three-Dimensional Bulk Heterojunction Morphology for Achieving High Internal Quantum Efficiency in Polymer Solar Cells. 19(15), pp. 2398-2406.

Kim, J. Y. et al., 2007. Efficient Tandem Polymer Solar Cells Fabricated by All-Solution Processing. *Science,* 317(5835).

Kin, L.-c.et al., 2020. Efficient Area Matched Converter Aided Solar Charging of Lithium Ion Batteries Using High Voltage Perovskite Solar Cells. *ACS Applied Energy Materials,* 3(1), pp. 431-439.

Kin, L.-C.et al., 2022. Efficient indoor light harvesting with CH3NH3Pb(I0.8Br0.2)3 solar modules and sodium-ion battery. *Cell Reports Physical Science,* 3(11), p. 101123.

Kondolot Solak, E. & Irmak, E., 2023. Advances in organic photovoltaic cells: a comprehensive review of materials, technologies, and performance. *RSC Advances,* pp. 12244-12269.

L. Cutting, C., Bag, M. & Venkataraman, D., 2016. Indoor light recycling: a new home for organic photovoltaics†. *Journal of Materials Chemistry C,* pp. 10367-10370.

Lechêne, B. P. et al., 2016. Organic solar cells and fully printed super-capacitors optimized for indoor light energy harvesting. *Nano Energy,* Band 26, pp. 631-640.

Lee, J.-H.et al., 2023. Recycling the Energy of Indoor Light: Highly Efficient Organic Photovoltaics via a Ternary Strategy. *ACS Applied Polymer Materials,* 5(6), pp. 4199-4209.

Li, B., Hou, B. & Amaratunga, G. A. J., 2021. Indoor photovoltaics, The Next Big Trend in solution-processed solar cells. *InfoMat,* 3(5), pp. 445-459.

Li, B., Hou, B. & Amaratunga, G. A. J., 2021. Indoor photovoltaics, The Next Big Trend in solution-processed solar cells. *InfoMat,* 3(5), pp. 445-459.

Li, G., Zhu, R. & Yang, Y., 2012. Polymer solar cells. *Nature Photonics,* 6(3), pp. 153-161.

Liu, L., Liu, W., Zhang, X. & Ingenhoff, J., 2019. Research on the novel explicit model for photovoltaic I-V characteristic of the single diode model under different splitting spectrum. *Results in Physics,* Band 12, pp. 662-672.

Loo, M., 2016. *Solar energy.* [Online]
Available at: http://maxloosolarenergy.blogspot.com/2016/12/series-and-shunt-resistance.html
[Zugriff am 21 07 2023].

Lübke, D., Hartnagel, P., Angona, J. & Kirchartz, T., 2021. Comparing and Quantifying Indoor Performance of Organic Solar Cells. *Advanced Energy Materials,* 11(34), p. 2101474.

Mathews, I., Kantareddy, S. N., Buonassisi, T. & Peters, I. M., 2019. Technology and Market Perspective for Indoor Photovoltaic Cells. *Joule,* 3(6), pp. 1415-1426.

Minnaert, B. & Veelaert, P., 2014. A Proposal for Typical Artificial Light Sources for the Characterization of Indoor Photovoltaic Applications. *Energies,* 7(3), pp. 1500-1516.

Mori, S. et al., 2015. Investigation of the organic solar cell characteristics for indoor LED light applications. *Japanese Journal of Applied Physics,* 54(7), p. 071602.

Mustafa, R. J., Gomaa, M. R., Al-Dhaifallah, M. & Rezk, H., 2020. Environmental Impacts on the Performance of Solar Photovoltaic Systems. *Sustainability,* 12(2), p. 608.

Nelson, J., 2011. Polymer:fullerene bulk heterojunction solar cells. *Materials Today,* 14(10), pp. 462-470.

Opoku, H., Hyeon Lee, J., Won Shim, J. & Woong Jo, J., 2022. Perovskite Photovoltaics for Artificial Light Harvesting. *Chemistry – A European Journal,* Band 28, p. e202200266.

PV.education, 2023. *PV.education.* [Online]
Available at: https://www.pveducation.org/pvcdrom/solar-cell-operation/open-circuit-voltage
[Zugriff am 30 07 2023].

Rau, U., 2023. *Photovoltaics II Characterisation and Simulation of Solar Cells.* s.l., Forschungszentrum Jülich.

Reinders , A., Verlinden, P., Sark, V. W. & Freundlich, A., 2017. *Photovoltaic solar energy , from fundamentals to applications.* Chichester, West Sussex, United Kingdom ; Hoboken, NJ: John Wiley & Sons, Ltd.

Scharber, M. C. & Sariciftci, N. S., 2013. Efficiency of bulk-heterojunction organic solar cells. *Progress in Polymer Science,* 38(12), pp. 1929-1940.

Shin, S.-C., You, Y.-J., Goo, J. S. & Shim, J. W., 2019. In-depth interfacial engineering for efficient indoor organic photovoltaics. *Applied Surface Science,* Band 495, p. 143556.

Sun, C. et al., 2022. LED-based solar simulator for terrestrial solar spectra and orientations. *Solar Energy,* Band 233, pp. 96-110.

Sun, L., Chen, Y., Sun, M. & Zheng, Y., 2023. Organic Solar Cells: Physical Principle and Recent Advances. *Chemistry – An Asian Journal,* 18(5), p. e202300006.

Swami, R., 2012. Solar Cell. *International Journal of Scientific and Research Publications,* .2(7).

Venkateswararao, A. et al., 2020. Device characteristics and material developments of indoor photovoltaic devices. *Materials Science and Engineering: R: Reports,* Band 139, p. 100517.

Wagner, M. et al., 2023. CO2 snow jet cleaning as a roll-to-roll compatible method for deburring IMI substrates after laser patterning. *Flexible and Printed Electronics,* 8(1).

Xie, L. et al., 2021. Recent progress of organic photovoltaics for indoor energy harvesting. *Nano Energy,* Band 82, p. 105770.

Xu, X. et al., 2021. An Overview of High-Performance Indoor Organic Photovoltaics. *ChemSusChem,* 14(17), pp. 3428-3448.

Yang, S.-S.et al., 2017. Toward High-Performance Polymer Photovoltaic Devices for Low-Power Indoor Applications. *Solar RRL,* 1(12), p. 1700174.

Yao, H. et al., 2016. Molecular Design of Benzodithiophene-Based Organic Photovoltaic Materials. *Chemical Reviews,* Band 116, pp. 7397-7457.

Yin, H. et al., 2018. Designing a ternary photovoltaic cell for indoor light harvesting with a power conversion efficiency exceeding 20%. *Journal of Materials Chemistry A,* 6(18), pp. 8579-8585.

Zhou, Y. et al., 2014. Efficient recyclable organic solar cells on cellulose nanocrystal substrates with a conducting polymer top electrode deposited by film-transfer lamination. *Organic Electronics*, 15(3), pp. 661-666.

ANNEX: Additional pictures

Solar simulator device

Sodium Na ion Battery Manufacturing Equipment

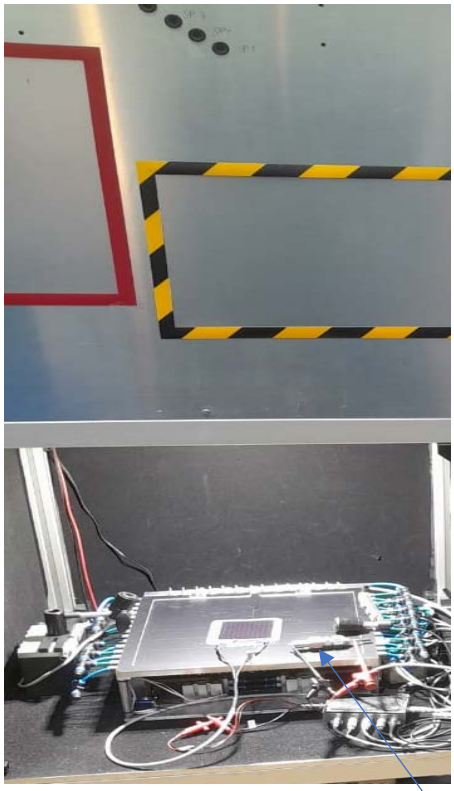

Sodium Na ion Battery

Sodium Na Battery couple direct couple direct With Opv Under LED 300-500 Lux image